A Dynamical Model of Subjectivity: Toward an Integrative Computational Architecture for the Mind

Takeo Imaizumi*

Independent Researcher, Kyoto City, Japan

Abstract

Subjective experience unfolds continuously yet also makes discrete, qualitative jumps. To model this phenomenological duality, we propose a discrete dynamical system. This yields a control-theoretic framework governed by a Mind Topography Map (MTM) of affective gain G and cognitive bias μ . The MTM's structure is isomorphic to a cusp catastrophe. Allowing negative gain (G < 0) generates error-amplifying loops that produce bistability, hysteresis, and period-doubling bifurcations. A key insight is that psychological stability is implementation-dependent. This analysis reveals a distinct zero-inertia state: the Ideal Dynamical Equilibrium (IDE).

To account for the mind's complexity, we extend the model into a multidimensional framework termed Structural Gain-Bias Dynamics (SGBD). This extension resolves a fundamental computational duality of mental life: how stable psychological "states" can coexist with persistent "processes" such as rumination. We show that this computational duality emerges from the interaction matrix's symmetric (state-seeking) and skew-symmetric (process-sustaining) components. We term this principle Cognitive Phase Dynamics (CPD).

To ground the framework empirically, we introduce two dimensionless indicators: D_{IDE} to quantify the balance between inertia and responsiveness, and D_{CPD} to distinguish states from processes. Supported by these metrics, our model serves as a computational bridge between the physics of the Free Energy Principle (FEP) and the teleology of Perceptual Control Theory (PCT). It thus offers a tractable and testable program for the future of mathematical psychology and computational psychiatry.

Keywords: Subjectivity, Discrete Dynamical Systems, Bifurcation Theory, Mathematical Psychology, Computational Psychiatry, Cognitive Architecture, Free Energy Principle (FEP), Perceptual Control Theory (PCT)

Contents

1	Introduction 1.1 The Phenomenological Duality of Subjectivity and the Dynamical Systems Perspective 1.2 Positioning the Model Within Foundational Theories	4
2	A Control-Theoretic Formulation of the Scalar Model 2.1 A Control-Theoretic Blueprint for Subjectivity	6 7
3	Discrete Dynamics in a Continuous Framework: Implementation-Dependent Stability 3.1 Two Core Propositions of the Subjectivity Model	8 8 9 9
4	Analysis of the Scalar Model: The Mind Topography Map 4.1 The MTM as a Cusp Catastrophe 4.2 Negative Affective Gain and Error-Amplifying Dynamics 4.3 A Quadrant-Based Analysis of the G-\(mu\) Plane 4.4 Representative Dynamics on the MTM: Simulation Cases 4.5 Dynamics of a Navigated Trajectory: A Simulation Case	10 10 10
5	From States to Processes: The Multidimensional SGBD Framework 5.1 Extension to a Multidimensional Framework 5.2 The Subjectivity Vector and Its Structure 5.3 Decomposition of Dynamics: States and Processes 5.3.1 A Mechanistic Duality in Dynamics: Introducing Cognitive Phase Dynamics (CPD) 5.3.2 CPD Indicator: "States" vs. "Processes" 5.3.3 A Two-Dimensional Cognitive Map: Linking IDE and CPD 5.4 A Taxonomy of Psychodynamics 5.5 A Dynamic Reinterpretation of Russell's Circumplex Model	12 12 13 13 13 14
6	The Trinity Architecture: An Integrative Framework for FEP and PCT 6.1 An Architecture of Three Interacting Layers	15 15 15
7	General Discussion7.1Summary of Theoretical Contributions	16 16 17 17
8	Conclusion	18

Call for Collaboration	19
Declarations	19
References	20
Tables	22
Figures	29
Appendices	34
Appendix A Mathematical Foundations of the Model	34
Appendix A.1 The Core Scalar Model	
Appendix A.1.1 Implementation Styles and Eigenvalue Mapping	
Appendix A.1.2 Bifurcation and Stability Analysis	
Appendix A.2 The Multidimensional SGBD Framework	35
Appendix A.2.1 Derivation of the Multidimensional Update Rule	35
Appendix A.2.2 Decomposition of WFe and Properties of the Dynamical System	36
Appendix A.2.3 Dynamic Attractors and the Neimark–Sacker Bifurcation	
Appendix A.2.4 Derivation of the Vectorized IDE State	
Appendix A.3 A Bayesian Model of the Self-System S	
Appendix A.3.1 Tactical Control (Fast Timescale)	
Appendix A.3.2 Strategic Learning (Slow Timescale)	
Appendix A.3.3 Implementation and Inference	38
Appendix B Connection to Cusp Catastrophe Theory	38
Appendix C Conceptual Application to Neurodevelopmental Disorders (NDDs)	39
Appendix C.1 Purpose and Positioning	
Appendix C.2 A Dynamic Reinterpretation of NDDs	
Appendix C.2.1 A State-Dominant Signature: Autism Spectrum Disorder (ASD)	
Appendix C.2.2 A Process-Dominant Signature: Tic Disorders and Rumination	
Appendix C.2.3 A Meta-Control Instability Signature: ADHD	
Appendix C.3 Prospects for Hypothesis Testing and Intervention	40 40
Appendix V. 4 – Lusciamer	411

1. Introduction

1.1. The Phenomenological Duality of Subjectivity and the Dynamical Systems Perspective

As James (1890) observed, subjective experience unfolds as both a continuous *stream of consciousness* and as discontinuous *moments*—sudden insights or shifts in mood. This phenomenological duality highlights a theoretical gap between the presumed continuity of neural and cognitive processes and the apparent discreteness of psychological state transitions.

An early and influential attempt to account for such discontinuity from the perspective of nonlinear dynamics was catastrophe theory (Thom, 1975), which formalized how continuous variations in input can yield abrupt, qualitative changes in a system's state. Walter J. Freeman later grounded this framework in neurophysiology, conceptualizing the brain as a self-organizing dynamical system in which transitions between meanings occur as discontinuous "jumps" rather than gradual shifts (Freeman, 2000). Extending this line of thought, we seek a computational mechanism that can generate the kind of discontinuous transitions Freeman described, advancing the theoretical lineage through a mathematically verifiable model.

This phenomenological duality also reveals a deeper tension between the objective description of neural processes and the subjective texture of lived experience. While bridging this divide remains one of the grand challenges of science, the present work takes a concrete step toward that goal by proposing a testable mathematical formulation. This historical and philosophical backdrop motivates our development of a formal framework, which we now situate within contemporary theories of cognition and consciousness.

1.2. Positioning the Model Within Foundational Theories

Current research on consciousness encompasses a diverse landscape of theories, broadly divided into those concerned with the ontology of consciousness (what it is) and those focused on its process (how it operates).

Among the ontological approaches, *Integrated Information Theory* (IIT) (Tononi, 2004) offers a rigorous account of the causal structure underlying conscious experience. However, IIT's primary emphasis lies on static causal architectures, leaving the temporal dynamics of subjective state transitions largely unexplored.

In contrast, process-oriented frameworks such as the Free Energy Principle (FEP) (Friston, 2010), Perceptual Control Theory (PCT) (Powers, 1973), and Global Workspace Theory (GWT) (Baars, 1988) illuminate the dynamic organization of cognition. Yet these approaches share a common limitation: their formulations typically rely on continuous-time dynamics, making it difficult to capture the qualitative "leaps" or structural reorganizations characteristic of psychological change. This tension is particularly salient when comparing the smooth, gradient-like dynamics of FEP with the discrete reorganizations central to PCT. While FEP, through the framework of Active Inference, allows for discrete policy selection, its foundational dynamics remain inherently continuous.

Our framework aims to resolve this limitation by introducing a computational architecture that gives rise to discrete transitions from an underlying continuous substrate. Rooted in *Dynamical Systems Theory* (DST) in cognition (van Gelder, 1995b), our model diverges structurally from previous approaches, offering a bridge between continuous neural processes and discrete psychological dynamics. The specific contributions of this framework are detailed in the following section.

1.3. Key Contributions of the Proposed Framework

In examining the complex phenomenon of subjectivity, this paper adopts a two-stage approach. First, we introduce a scalar model that abstracts the *core principles* of subjectivity at a high level of generality. Insights from this model then inform its *extension* into a multidimensional framework capable of capturing more intricate features, including individual differences. Guided by this design philosophy, the specific contributions of the paper can be summarized in the following six points:

- A Basic Mechanism of Subjectivity: Introducing the *Mind Topography Map* (MTM)—a phase diagram of subjectivity isomorphic to a cusp catastrophe—which formalizes the error-amplifying dynamics underlying various forms of psychopathology.
- A New Dynamical State of Equilibrium: Defining the *Ideal Dynamical Equilibrium* (IDE), a distinctive zero-inertia state, and proposing a testable metric, D_{IDE} , to quantify the balance between inertia and responsiveness.

- A Structural Model of the Inner World: Developing the multidimensional Structural Gain-Bias Dynamics (SGBD) framework to computationally represent complex mental organizations such as internal conflict.
- A Core Mechanism for States and Processes: Introducing Cognitive Phase Dynamics (CPD) as a unifying principle for the dynamics of stable psychological states and persistent processes (e.g., rumination), supported by the testable indicator D_{CPD} .
- A Methodological Foundation for Discrete Dynamics: Reframing the relation between continuous theories and discrete events as an *implementation problem*, revealing that psychological stability depends on individual cognitive style and temporal rhythm.
- An Integrated Cognitive Architecture: Proposing the *Trinity Architecture* as a computational bridge linking the physical causality of the FEP with the teleological normativity of PCT.

1.4. Structure of This Paper

This paper is organized to develop the theoretical framework in a stepwise manner. The first half establishes the core single-variable model: Section 2 formulates its control-theoretic foundation and identifies the IDE state; Section 3 presents the "Discrete-in-Continuous" perspective; and Section 4 examines the model's dynamics through the MTM.

The second half extends this foundation. Section 5 introduces the multidimensional SGBD framework to account for both psychological "states" and "processes," while Section 6 situates this framework within the integrative Trinity Architecture, linking FEP and PCT.

Finally, Section 7 summarizes the main contributions, discusses limitations, and outlines directions for future research. The appendices provide additional support: Appendix A elaborates on the mathematical foundations, Appendix B clarifies the connection to cusp catastrophe theory, and Appendix C presents a conceptual application.

2. A Control-Theoretic Formulation of the Scalar Model

2.1. A Control-Theoretic Blueprint for Subjectivity

The conceptual starting point and central hypothesis of this paper is the control-theoretic blueprint for subjectivity illustrated in Figure 1. While previous models have explored feedback systems in the mind, this framework is novel in its explicit positioning of objective and subjective states and its integration of cognitive bias and affective gain into a mathematically tractable feedback architecture.

Modeling this comprehensive blueprint in its entirety is a formidable challenge. Therefore, as a crucial first step, this paper focuses on analyzing the dynamics of the core internal loop of subjectivity—the subsystem enclosed by the dotted line. By isolating this computational "engine," we aim to derive the fundamental principles governing subjective experience, thereby laying the groundwork for the future research directions outlined in Subsection 7.4.

This blueprint comprises the following main components:

- External/Internal World: The external physical and social environment, and the internal mental domain where an individual's objective state (M_o) and subjective state (M_s) are defined.
- Filter Bank (F_r, F_i, F_e) : Functional modules responsible for different stages of information processing, such as recognition, interpretation, and evaluation.
- Objective State (M_o) : A representation of the external world, derived through the recognition filter (F_r) . It contrasts with the subjective state (M_s) .
- Subjective State (M_s) : A representation within the individual's internal mental world, shaped by their perception and interpretation of reality. It contrasts with the objective state (M_o) .
- Error (e): The discrepancy between the objective and subjective states ($e = M_o M_s$), serving as the driving force for updating the subjective state (M_s).
- Cognitive Bias (μ): A persistent tendency that attracts or repels the subjective state in a particular direction. Beliefs, memories, and values are included in this category.
- **Process Noise** (ε): Transient noise that perturbs the subjective state.

- Mental Fluctuation (ω): Internal perturbation, where $\omega = \mu + \varepsilon$ (cognitive bias + process noise), that augments the output of the Evaluation Filter (F_e).
- Affective Gain (G): A coefficient representing the system's sensitivity to the combined signal from the Evaluation Filter (F_e) and Mental Fluctuation (ω) , dynamically modulating its influence.
- Self-System (S): A higher-order control element that dynamically adjusts the system's parameters, including (G) and (μ) . It can be regarded as a central component of subjectivity, responsible for learning, adaptation, and decision-making.
- Action (A): The action generated toward the external world in response to the update signal of the subjective state (M_s) .

A key distinction from PCT lies in the nature of the target state. Whereas PCT's "reference signal" represents an internal goal to be achieved, our objective state M_o corresponds to an external reality that functions as an attractor. This difference is crucial: PCT models error minimization with respect to an internal standard, while our framework explains how subjective state M_s can reach a stable equilibrium at a finite distance from external reality, anchored by the cognitive bias μ . This enables the modeling of phenomena in which subjectivity systematically diverges from objectivity—from wishful thinking to paranoia.

From this blueprint, the signal for updating the subjective state M_s can be expressed in its most general form as follows. This equation serves as the theoretical starting point:

Update Signal(t) =
$$G(S,t)$$
 [$F_e(M_o(t) - M_s(t), S, t) + \mu(S,t) + \varepsilon(S,t)$] (1)

This equation indicates that the gain G, bias μ , process noise ε , and evaluation filter F_e are dynamic quantities that may vary over time under the modulation of the self-system S. A list of the main symbols used in this paper is provided in Table 1. While this general form captures the system's full complexity, a more tractable formulation is required to analyze its core dynamics; the next section introduces the simplifying assumptions made for this purpose.

2.2. The Continuous-Time Stochastic Differential Equation

To refine the general form in Equation (1) into a tractable model of the system's core dynamics, we introduce four standard assumptions:

- Assumption 1: Standardized Objective Model: The objective state is set to zero $(M_o \equiv 0)$ to isolate the system's intrinsic dynamics.
- Assumption 2: Linear Evaluation Filter: The evaluation filter is assumed to be linear, $F_e(e) = e$. While this scalar simplification is essential for the foundational model, the internal *structure* of this filter will be elaborated in the multidimensional extension (Section 5).
- Assumption 3: Fixed Parameters: The affective gain G and cognitive bias μ are treated as fixed parameters, temporarily disregarding their adaptive modulation by the self-system S.
- Assumption 4: Nonlinear Saturation: To capture biological constraints that prevent unbounded growth (e.g., neural saturation), a standard nonlinear saturation term $-\alpha M_s^3$ (where $\alpha > 0$) is introduced, acting as a restoring force (Strogatz, 2018).

Under these assumptions, the rate of change of the subjective state, dM_s/dt , can be expressed as:

$$\frac{\mathrm{d}M_s(t)}{\mathrm{d}t} = G(-M_s(t) + \mu) - \alpha M_s(t)^3 + G\varepsilon(t)$$

Formalizing the process noise term $G\varepsilon(t)$ as a Wiener process dW_t with intensity σ , we obtain the model's foundational Stochastic Differential Equation (SDE):

$$dM_s(t) = \left(-GM_s(t) - \alpha M_s(t)^3 + G\mu\right) dt + G\sigma dW_t \tag{2}$$

The properties of this SDE, including its stationary variance, are detailed in Subsubsection Appendix A.1.1. This equation serves as the continuous-time theoretical foundation from which our discrete implementation is derived.

2.3. The Implementation Problem: From Continuous Theory to Discrete Reality

An abstract continuous theory must ultimately be instantiated in a physical system such as the brain, which operates through discrete events. This gives rise to an often-overlooked theoretical challenge that we term the *implementation problem*. Any realization of a continuous theory requires temporal sampling, and the choice of sampling scheme profoundly shapes the resulting dynamics.

To formalize this, we discretize the SDE (Equation (2)) using a fundamental implementation approach: the forward Euler method for the deterministic component and the Euler–Maruyama method for the stochastic component. For simplicity, the time step is set to $\Delta t = 1$.

First, the deterministic skeleton of the system yields the fixed-point equation describing its stable equilibria (M_s^*) :

$$\alpha (M_s^*)^3 + GM_s^* - G\mu = 0 \tag{3}$$

Second, the stochastic Wiener process term $G\sigma$ d W_t becomes a discrete process noise term $G\varepsilon(t)$, where $\varepsilon(t)$ is drawn from a standard normal distribution scaled by σ .

Combining these components produces the core update rule for subjective dynamics—a discrete map that serves as the central mechanism of our model:

$$M_{s,t+1} = (1 - G)M_{s,t} - \alpha M_{s,t}^3 + G\mu + G\varepsilon(t)$$

$$\tag{4}$$

Together, Equation (3) defines the stability landscape (the MTM), while Equation (4) governs the system's evolution upon it. This pair of equations constitutes the mathematical mechanism of our model. The next section examines a key insight that emerges from analyzing its linear properties.

2.4. The Ideal Dynamical Equilibrium (IDE) State

A close examination of the core update equation, Equation (4), reveals a crucial insight. The linear autoregressive coefficient (1-G) determines how strongly the previous state $M_{s,t}$ influences the next state $M_{s,t+1}$. This term represents the system's cognitive inertia—its intrinsic tendency to carry forward its prior momentum. The behavior of this inertia term at two singular parameter values, G=0 and G=1, exposes a fundamental distinction between dynamic regimes.

When G=0, the system becomes purely inertial, effectively disconnected from both the cognitive bias μ and process noise $\varepsilon(t)$. The update equation simplifies to $M_{s,t+1}=M_{s,t}-\alpha M_{s,t}^3$, reducing the system to a deterministic echo of its past. In contrast, when G=1, the inertia term (1-G) vanishes entirely. The system's linear memory is erased, enabling perfect responsiveness to current inputs $(\mu$ and $\varepsilon(t))$. We refer to this unique, zero-inertia state as the *Ideal Dynamical Equilibrium (IDE)*. The key functional distinctions between these two regimes are summarized in Table 2.

The IDE state is not merely a mathematical abstraction. Its properties—a dynamic balance between stability and immediate responsiveness—resonate with psychological notions of mindfulness. For instance, the emphasis on the "here and now" in contemplative traditions such as Zen and the Middle Way reflects a mental state free from attachment to the past (cognitive inertia) and highly responsive to the present moment (Tang et al., 2015). The term "Ideal" is thus employed in a technical rather than normative sense, denoting a condition of pure responsiveness. Identifying this functionally significant equilibrium motivates a deeper exploration of its properties and the conditions under which it emerges—a topic addressed in the following section.

3. Discrete Dynamics in a Continuous Framework: Implementation-Dependent Stability

3.1. Two Core Propositions of the Subjectivity Model

We formalize the relationship between our discrete model and its continuous origin—a viewpoint we term the *Discrete-in-Continuous perspective*—to ensure the model is both faithful to the theory and offers new insights. This formalization rests on the following two core propositions.

For $G = 1, \mu = 0$, although f'(0) = 0, the zero fixed point remains stable with cubic convergence due to $x_{t+1} = -\alpha x_t^3$. We formalize this concept operationally in Definition IDE.

Proposition 1 (Equilibrium Equivalence). In short: The system's stable "resting points" occur at the same locations in both the continuous theory and the discrete model.

The set of fixed points of the discrete map is identical to the set of equilibria of the original continuous system, provided that the discretization method is fixed-point preserving.²

Proposition 2 (Implementation-Dependent Stability). In short: Even if a resting point exists, whether the system can actually "remain" there depends on the implementation (e.g., cognitive style or rhythm).

The stability of a fixed point—and the bifurcations that arise from it—depend critically on the implementation details of the discretization (method H and timestep Δt). Local stability holds when $|\lambda_d(\lambda_c; H, \Delta t)| < 1$, where the mapping from the continuous eigenvalue λ_c to the discrete eigenvalue λ_d is specific to the chosen implementation scheme H.³

These propositions are grounded in standard principles of dynamical systems theory (see Subsubsection Appendix A.1.1). Their key implication—particularly that of Proposition 2—is that psychological stability is not intrinsic but emergent. This reveals that, for the same underlying conflict (an unstable continuous eigenvalue λ_c), the psychological outcome—whether a thought remains a stable concern or escalates into rumination—can depend entirely on an individual's cognitive style (implementation method H) or rhythm (timescale Δt) (Kuznetsov, 2004; Guckenheimer and Holmes, 1983; Strogatz, 2018).

3.2. Theoretical Rationale for a Discrete-Time Model

Our adoption of a discrete-time model is not merely an approximation but a core theoretical commitment. Although it originates from a continuous SDE, we argue that the dynamics emerging from its discrete implementation are not numerical artifacts to be minimized, but rather the very source of the model's explanatory power for subjectivity.

The significance of this choice is substantial. As shown in Tables 3 and 4, the differing stability criteria of discrete maps ($|\lambda_d| < 1$) and continuous flows ($\text{Re}(\lambda_c) < 0$) enable a richer repertoire of dynamic behaviors. In particular, our discrete framework gives rise to two key phenomena that are impossible in its one-dimensional continuous counterpart:

- 1. **Period-doubling (flip) bifurcations**, providing a direct mechanistic basis for oscillatory states such as rumination and for the sudden onset of psychological instability.
- 2. **The IDE**, a unique zero-inertia state of perfect responsiveness that cannot be captured by continuous dynamics.

It is precisely these implementation-dependent phenomena that offer a new lens through which to understand the mind. Thus, we embrace the discrete framework not as a surrogate for continuous theory, but as an indispensable tool for revealing dynamics that would otherwise remain hidden.

3.3. The Canonical Skeleton of Discrete Dynamics

Having established the theoretical necessity of adopting a discrete perspective, we now generalize our model to show that it rests upon a canonical computational skeleton. This generalization enables us to move from a bottom-up observation derived from a specific implementation to a top-down formulation of a potentially canonical principle. We specialize this general form into the following canonical structure, whose coefficients Φ_H and Γ_H explicitly capture the implementation-dependent dynamics of inertia and drive:

$$M_{s,t+1} = \underbrace{\Phi_H(G,\Delta t)M_{s,t}}_{\text{Inertia}} + \underbrace{\Gamma_H(G,\Delta t)\,\mu}_{\text{Drive}} + \underbrace{\text{(nonlinear term)}}_{\text{Saturation}} + \underbrace{\text{(process noise)}}_{\text{Fluctuation}}$$
(5)

This "inertia + drive + saturation" structure is a ubiquitous mathematical form. It constitutes the backbone of the discrete-time state-space model in control engineering $(x_{k+1} = Ax_k + Bu_k)$ and parallels

²A method is fixed-point preserving if an equilibrium of the continuous system is always a fixed point of the discrete map, and vice versa.

³Here, λ_c and λ_d denote the eigenvalues of the system's Jacobian matrix at the fixed point for the continuous and discrete systems, respectively. The stability criteria are $\text{Re}(\lambda_c) < 0$ for continuous systems and $|\lambda_d| < 1$ for discrete maps.

the hidden-state update equation of a recurrent neural network (RNN) $(h_t = f(W_{hh}h_{t-1} + W_{xh}x_t))$. By grounding our psychological model explicitly in this canonical skeleton, we can articulate two novel principles that extend from it:

- 1. Allowance for Negative Gain. We explicitly permit negative affective gain (G < 0), which provides the core mechanism for modeling a range of pathological dynamics, as demonstrated in Subsection 4.2.
- 2. Implementation-Dependent Stability. We propose that psychological stability is not intrinsic but depends on cognitive implementation, which predicts the emergence of unique states such as the IDE from specific cognitive styles H and rhythms Δt .

The following section details the dynamical phenomena that arise from these implementation details.

3.4. IDE as an Implementation-Dependent Principle

This section explores a key implication of implementation-dependent stability: that variations in cognitive style H and rhythm Δt shape the system's dynamics. To analyze this, we define the dimensionless product $\kappa := G \Delta t$ as the key control parameter. The most significant consequence is that the IDE is not a universal feature but an emergent state dependent on the specific implementation, as we now formalize:

Definition IDE (Operational Definition of IDE). The IDE is a singular state of pure responsiveness characterized by two conditions: the absence of directional bias ($\mu = 0$) and the complete disappearance of linear cognitive inertia ($\Phi_H(\kappa) = 0$). The precise conditions for realizing this zero-inertia state are implementation-dependent, as illustrated in Table 5 and Figure 2.

3.4.1. IDE Indicator: "Inertia" vs. "Responsiveness"

To translate this principle into a testable scientific claim, we introduce a dimensionless indicator. Following a long scientific tradition of employing such ratios to characterize complex systems (e.g., the Reynolds number), D_{IDE} quantifies the balance between cognitive inertia and responsiveness.

Indicator 1 (IDE indicator D_{IDE}).

$$D_{\text{IDE}} := \frac{\left| \partial M_{s,t+1} / \partial M_{s,t} \right|}{\left| \partial M_{s,t+1} / \partial \mu \right|} \Big|_{M_s = 0, \mu = 0} = \frac{\left| \Phi_H(\kappa) \right|}{\left| \Gamma_H(\kappa) \right|}. \tag{6}$$

This indicator is non-negative, with a theoretical range of $[0, \infty)$.

The indicator becomes zero ($D_{\text{IDE}} = 0$) precisely at the IDE state, where $\Phi_H(\kappa) = 0$. From a psychological perspective, the parameters that constitute this indicator offer a fertile ground for interpretation. The timescale Δt can be viewed as a manipulable "cognitive rhythm," while the implementation style H can be understood as a stable "cognitive style." For instance, a simple implementation scheme (e.g., forward Euler) can be seen as paralleling fast, intuitive reasoning, whereas a more sophisticated one (e.g., Tustin) corresponds to deliberate, analytical processing.

This reinterpretation of engineering methodologies as "cognitive styles" lies at the core of our contribution. The discretization methods discussed here are, of course, standard tools in control engineering, traditionally employed to analyze system properties such as stability and frequency response (Franklin et al., 1998). Our novelty does not lie in the methods themselves, but in their conceptual recontextualization: rather than pursuing technical objectives such as controller design, we apply these methods from a psychological standpoint to investigate how different cognitive styles influence psychological stability.

4. Analysis of the Scalar Model: The Mind Topography Map

4.1. The MTM as a Cusp Catastrophe

Through our *Discrete-in-Continuous perspective*, we now explore the model's dynamics. To this end, we introduce the *Mind Topography Map* (MTM)—a central contribution of this paper (Figure 3). The MTM functions as a "phase diagram" of subjectivity, visualizing how affective gain G and cognitive bias μ jointly shape the landscape of stable states and pathological transitions.

The MTM's structure is rigorously grounded in catastrophe theory (Thom, 1975; Zeeman, 1977), as our model's equilibrium equation (Equation (3)) is mathematically isomorphic to a cusp catastrophe. This isomorphism confirms that G and μ act as its control parameters (see Appendix B). The map's boundaries are bifurcation curves defined by the discriminant of this equation. We use a reduced discriminant $\tilde{\Delta}$ to partition the MTM into distinct regions (see Table 6):

$$\tilde{\Delta} = -4G^3 - 27\alpha G^2 \mu^2. \tag{7}$$

Physically, the MTM can be viewed as a potential landscape where stable psychological states are "valleys" (Tanaka et al., 2019). However, this static analogy is incomplete; as established in Section 3, our discrete framework generates unique phenomena that have no counterpart in continuous flows. This critical distinction calls for a direct analysis of the model's dynamics, which we now undertake.

4.2. Negative Affective Gain and Error-Amplifying Dynamics

A key feature of our model is its allowance for negative affective gain (G < 0), which shifts the dynamics from healthy, error-correcting to pathological, error-amplifying ones. While DST has long examined such feedback as $unstable\ dynamics$ (van Gelder, 1995b,a), our discrete framework reveals specific consequences that continuous formulations cannot capture: a formal isomorphism to a $cusp\ catastrophe\ (Appendix\ B)$ and the emergence of period-doubling bifurcations. The most profound outcome of this error-amplifying dynamic is the creation of a bistable region on the MTM. This occurs because the nonlinear saturation term $(-\alpha M_s^3)$ constrains runaway growth, producing a landscape of new, distant attractors instead of unbounded divergence.⁴ This bistable landscape gives rise to history dependence, or hysteresis, which provides a computational account for self-reinforcing loops (e.g., "anxiety begets more anxiety") and explains clinically salient phenomena such as mood relapse and the persistence of cognitive biases. While this section focuses on the mechanistic consequences of negative gain, its broader implications will be discussed in Section 6.

4.3. A Quadrant-Based Analysis of the G-μ Plane

The MTM is best interpreted using the quadrant-based heuristic summarized in Table 7. This classification arises from the distinct roles of the two axes: affective gain G functions as the system's primary dynamic switch, toggling between an error-correcting regime (G>0) and an error-amplifying one (G<0), while cognitive bias μ sets the system's target. The critical insight from this analysis is the asymmetry it reveals: while the adaptive region (G>0) captures stable goal pursuit, it is the escapist region (G<0) that produces the complex, history-dependent dynamics (e.g., hysteresis) essential for modeling persistent maladaptive states.

4.4. Representative Dynamics on the MTM: Simulation Cases

To ground the MTM's abstract topology in observable behavior, we now simulate its dynamics at four representative points on the map (Figure 3), governed by the update rule in Equation (4).⁵

Adaptive, High Sensitivity (G > 1) With parameters G = 1.5 and $\mu = \pm 0.5$, placing the system in the monostable region, the subjective state converges steeply toward the bias, modeling an overly sensitive or hyper-responsive cognitive style (Figure 4).

Adaptive, Standard (0 < G < 1) With parameters G = 0.3 and μ = \pm 0.5, also in the monostable region, the state converges more gradually to the bias, representing a moderate and stable adaptive dynamic characteristic of healthy learning (Figure 5).

Escapist, Bistable (G < 0) With parameters G = -0.5 and $\mu = \pm 0.5$, placing the system in the bistable region, a single trajectory is captured by one of two distinct attractors, demonstrating history dependence (Figure 6). The existence of this dual-attractor structure is statistically confirmed by the bimodal distribution that emerges in long-term simulations (Figure 7).

⁴The coexistence of an amplifying force and a nonlinear containing force is a standard feature of DST models of selforganization, evident in mechanisms ranging from logistic growth to the saturating activation functions of neural networks.

⁵In all simulations, the nonlinear saturation coefficient was set to $\alpha = 0.1$ and the process noise intensity to $\sigma = 0.05$.

The IDE State $(G = 1, \mu = 0)$ At this unique point within the monostable region, linear inertia vanishes. The state exhibits a perfect balance between stability and responsiveness, agilely tracking process noise without being captured by it—embodying a centered state of mind (Figure 8).

A comparison of the two regimes reveals the model's most critical dynamic: the belief amplification effect. Whereas the adaptive region (G > 0) causes the subjective state M_s to converge directly to the bias μ , the escapist region (G < 0) amplifies a mild bias $(|\mu| = 0.5)$ into a strong, stable conviction with a magnitude $(|M_s|)$ of 2.0 to 2.5, as shown in Figure 6. This amplification is not unbounded; the error-amplifying feedback from G < 0 is constrained by the nonlinear saturation term, which carves out new, distant attractors in the system's landscape.

The underlying probability landscape in Figure 7 reveals the origin of this effect: a dual asymmetry in the attractors' locations and probabilities. This symmetry breaking is caused by the constant force from the $G\mu$ term, which simultaneously shifts the attractors' positions and tilts the potential landscape. A positive bias $(\mu > 0)$, for example, draws the corresponding positive attractor closer to the origin $(M_s \approx 2.0)$ while deepening its basin of attraction, thereby increasing its likelihood. This mechanism provides a formal computational account of how a minor cognitive bias can evolve into a deeply entrenched and nuanced pathological fixation.

4.5. Dynamics of a Navigated Trajectory: A Simulation Case

Having analyzed the system's behavior under fixed parameters, we now provide a proof of concept illustrating the self-system S and its role in active self-regulation. This simulation demonstrates how S can dynamically adjust the affective gain G and cognitive bias μ to navigate the MTM, transitioning through distinct psychological states. The spiral trajectory plotted on the map in Figure 3 unfolds as a compelling mental journey comprising three phases (Figure 9).

- Phase 1: Adaptive Tracking (Timesteps 0–400) The journey begins in the adaptive, monostable region (G > 0). Here, the subjective state $M_s(t)$ effectively tracks the evolving negative bias $\mu(t)$, demonstrating a flexible and proportionate response to shifting internal conditions.
- Phase 2: Pathological Fixation (Timesteps 400–700) As the parameters move into the escapist, bistable region (G < 0), a catastrophic bifurcation occurs around timestep 400. The subjective state $M_s(t)$ detaches from the bias and locks into the *belief amplification* dynamic. This pathological state becomes self-sustaining through hysteresis, persisting even after the bias $\mu(t)$ reverses sign.
- Phase 3: Recovery and Centering (Timesteps 700–1000) Upon re-entering the adaptive, monostable region (G > 0) near timestep 700, the system escapes the pathological attractor and rapidly reconverges with the bias. The self-system then guides both parameters toward the IDE point $(G = 1, \mu = 0)$, achieving a stable, centered equilibrium.

This trajectory unifies a full psychological cycle—from healthy adaptation and pathological fixation to recovery—into a single process of self-regulation. It demonstrates how the self-system S navigates the MTM's stability landscape to integrate these distinct mental states.

5. From States to Processes: The Multidimensional SGBD Framework

5.1. Extension to a Multidimensional Framework

While the preceding scalar model revealed a rich landscape of dynamics, its central limitation is its representation of subjectivity as a single variable M_s . To address this, we extend the core scalar update rule (Equation (4)) into a multidimensional form. This is achieved by replacing each scalar component—subjective state M_s , gain G, bias μ , saturation α , and noise ε —with its corresponding vector form, as detailed in Table 1. We term this multidimensional extension the *Structural Gain-Bias Dynamics* (SGBD) framework, designed to capture the intricate tapestry of the inner world, where multiple, often conflicting, mental states coexist.

5.2. The Subjectivity Vector and Its Structure

The true power of this vector representation lies in its ability to structure the high-dimensional subjective space into a set of psychologically meaningful subspaces. This elevates the model from a single point to a rich canvas upon which the architecture of the mind can be drawn.

Mathematically, this corresponds to partitioning the N-dimensional subjective vector \mathbf{M}_s into a collection of functionally distinct sub-vectors:

$$m{M_{\mathrm{sub}}}_1 = \left(egin{array}{c} m{M_{\mathrm{sub}}}_1 \ m{M_{\mathrm{sub}}}_2 \ m{M_{\mathrm{sub}}}_3 \ dots \end{array}
ight) egin{array}{c} N_1 ext{ dimensions} \ N_2 ext{ dimensions} \ N_3 ext{ dimensions} \end{array} \quad ext{such that } N = \sum_i N_i.$$

By assigning specific psychological meanings to each sub-vector, we can illustrate the expressive potential of this framework. For example, it can model:

- Hierarchical structures of the self, such as the interplay among sub-vectors representing the Freudian "superego," "ego," and "id" (Freud, 1923).
- An inner society of self and others, by placing sub-vectors for the "self" alongside those representing "internalized others," such as a demanding boss or an idealized mentor.
- Conflicts of value, by juxtaposing mutually exclusive goals—for instance, a sub-vector oriented toward "career success" and another toward "family time."

Thus, the vectorized framework provides the foundational blueprint for the mind's static architecture. Yet this remains only a schematic design. The critical question is: what constitutes the "mechanism" that drives the dynamics upon this blueprint?

5.3. Decomposition of Dynamics: States and Processes

The key to modeling these complex dynamics lies in a component of our initial blueprint (Figure 1): the Evaluation Filter (F_e) . In the foundational scalar model (Assumption 2), this filter was treated as a simple linear element, rendering it effectively invisible. In the SGBD framework, we lift this simplification by promoting F_e to a square matrix, termed the evaluation weight matrix, \mathbf{W}_{Fe} . Because this matrix governs the relationships among the dimensions of the subjective vector \mathbf{M}_s , it functions as the system's core interaction matrix. This innovation is powerful, as it allows us to model the rich structure of the inner world—a capability impossible in the scalar model. As detailed in Subsection Appendix A.2, this extension yields the general update equation for the SGBD framework, shown as Equation (8).

$$M_s(t+1) = M_s(t) - \alpha \odot (M_s(t))^{\circ 3} + G_{\text{eff}}(t) \odot (-W_{\text{Fe}}M_s(t) + \mu_{\text{eff}}(t) + \varepsilon(t))$$
(8)

A mathematical analysis of the force term $-\mathbf{W}_{\mathrm{Fe}}M_{\mathrm{s}}$ reveals a key insight. Although decomposing any square matrix into its symmetric (\mathbf{S}) and skew-symmetric (\mathbf{R}) components is a standard mathematical operation, its application to differentiate psychological "states" from "processes"—a perspective common in fields such as physics, engineering, and neuroscience (see Table 8)—has been largely overlooked in psychology. As we will demonstrate, these two components have fundamentally different dynamic roles that directly address our central question:

- The **symmetric component** (**S**) generates a *gradient force*. This force drives the system down the slope of a potential energy landscape toward a stable minimum. It produces convergence, corresponding to the formation of a psychological "state."
- The skew-symmetric component (R) generates a rotational force. Always orthogonal to the state vector, it performs no net work on the system but induces cyclic or orbital motion on the potential landscape. It produces persistence and recurrence, corresponding to a psychological "process."

This mechanistic duality—between gradient and rotational dynamics—maps directly onto a psychological one, separating state-seeking from process-sustaining forces. We hypothesize that the rotational forces generated by the skew-symmetric component are the computational manifestation of asymmetric relationships among psychological values. For example, a strong focus on "career success" may actively suppress the value

of "family time," whereas the reverse influence may be weaker or absent. It is precisely such hierarchical or one-way value interferences that the skew-symmetric component captures, giving rise to the dynamics of persistent trade-offs and unresolved inner conflicts.

5.3.1. A Mechanistic Duality in Dynamics: Introducing Cognitive Phase Dynamics (CPD)

We refer to this core principle—the conceptual distinction between gradient and rotational dynamics—as Cognitive Phase Dynamics (CPD). CPD offers a unified, mechanistic account of how a single cognitive architecture can accommodate both stable psychological phenomena, such as beliefs and moods, and persistent dynamic phenomena, such as rumination and creative thought.

5.3.2. CPD Indicator: "States" vs. "Processes"

This insight naturally raises a testable question: within any given mental state, what is the balance between these two forces? To quantify this relationship and render the CPD concept empirically verifiable, we introduce a dimensionless indicator.

Indicator 2 (CPD indicator D_{CPD}). Given the decomposition $\mathbf{W}_{Fe} = \mathbf{S} + \mathbf{R}$, with $\mathbf{S}^{\top} = \mathbf{S}$ and $\mathbf{R}^{\top} = -\mathbf{R}$, we define the CPD indicator as the dimensionless ratio

$$D_{\text{CPD}} := \frac{\|\mathbf{S}\|_F}{\|\mathbf{R}\|_F}.\tag{9}$$

Here, $\|\cdot\|_F$ denotes the Frobenius norm. In the special case where the rotational component is zero ($\|\mathbf{R}\|_F = 0$), as in a purely symmetric matrix, we define $D_{\text{CPD}} \equiv \infty$ to represent the absolute dominance of state-seeking dynamics. The indicator thus ranges theoretically over $[0,\infty]$. Values of $D_{\text{CPD}} > 1$ indicate S-dominant (state/gradient) dynamics, $D_{\rm CPD} < 1$ indicate R-dominant (process/rotational) dynamics, and $D_{\rm CPD} = 1$ marks the balance point between the two regimes.

For convenience, we also define a signed logarithmic version:

$$D_{\text{CPD,log}} := \log \frac{\|\mathbf{S}\|_F}{\|\mathbf{R}\|_F}.$$
 (10)

5.3.3. A Two-Dimensional Cognitive Map: Linking IDE and CPD

The two indicators introduced in this paper, D_{IDE} and D_{CPD} , can be combined to construct a twodimensional cognitive map. These indicators form two orthogonal⁶ axes that are semantically complementary: the $D_{\rm IDE}$ axis quantifies the balance between "inertia" and "responsiveness," while the $D_{\rm CPD}$ axis quantifies the balance between "state" and "process" dynamics.⁷ Together, these axes define a plane that allows the classification of four primary cognitive regimes:

- $D_{\text{CPD,log}} > 0, D_{\text{IDE}} > 0$: Rigid Beliefs A regime dominated by states and high inertia, leading to inflexible or dogmatic thinking.
- $D_{\text{CPD,log}} < 0, D_{\text{IDE}} > 0$: Rigid Rumination A regime dominated by processes and high inertia, characteristic of obsessive or depressive thought loops.
- $D_{\text{CPD,log}} > 0$, $D_{\text{IDE}} \approx 0$: Adaptive Goal-Focus A regime dominated by states and high responsiveness (low inertia), oriented toward stable goal attainment.
- $D_{\text{CPD,log}} < 0, D_{\text{IDE}} \approx 0$: Creative Exploration A regime dominated by processes and high responsiveness (low inertia), characterized by open-ended, rotational cognition.

The origin $(D_{\text{CPD,log}} \approx 0, D_{\text{IDE}} \approx 0)$ represents a notable synthesis: a highly adaptive condition that balances responsiveness with centered equilibrium.

⁶Here, "orthogonal" is used conceptually to indicate that the two indicators measure independent, non-redundant aspects of the system's dynamics.

Note that D_{IDE} is defined as a ratio of absolute values and is therefore always non-negative, whereas $D_{\text{CPD,log}}$ is a log-ratio

whose sign indicates which component $(S \text{ or } \mathbf{R})$ is dominant.

5.4. A Taxonomy of Psychodynamics

We now analyze how the symmetric (gradient) and skew-symmetric (rotational) forces arising from \mathbf{W}_{Fe} interact with the system's overall regime, determined by the sign of affective gain G (adaptive vs. escapist). This interaction yields four characteristic psychodynamic regimes, which are summarized in Table 9. Their qualitative dynamics are illustrated as vector fields in Figure 10, generated by the representative parameter sets in Table 10 (assuming $\mu_{\text{eff}} = \mathbf{0}$). The functional interpretation of each regime is outlined below.

- Healthy Conflict (Figure 10A): An adaptive, state-dominant system produces a stable saddle point, modeling a clear decision point that guides the state toward resolution.
- Severe Conflict (Figure 10B): An escapist, state-dominant system inverts stability, turning the origin into an unstable repeller. This captures a dissociative state in which the system cannot settle.
- Stable Rumination (Figure 10C): An adaptive, process-dominant system exhibits a stable spiral convergence, modeling a manageable cognitive process that culminates in resolution.
- Catastrophic Rumination (Figure 10D): An escapist, process-dominant system shows an unstable spiral divergence, which—when extended to the full nonlinear model—manifests as a limit cycle, modeling a self-sustaining vicious loop of thought.

5.5. A Dynamic Reinterpretation of Russell's Circumplex Model

To demonstrate the utility of the psychodynamic taxonomy, we apply it to a classic model in affective science: Russell's circumplex model of affect (Russell, 1980), a foundational framework that maps emotions onto a two-dimensional space defined by Valence and Arousal. The synergy is evident: the circumplex model provides an empirical description of what emotions are, whereas our SGBD framework offers a mechanistic account of how they behave.

This complementarity enables new explanations for complex emotional phenomena that static maps cannot capture:

- The Paradox of Happiness: Why can the deliberate pursuit of happiness lead to greater unhappiness? Our framework explains this through the S-dominant escapist regime (Figure 10B). When the goal of "being happy" is pursued under an escapist gain (G < 0), it becomes an unstable repeller, driving the subjective state away from the desired emotion.
- Vicious Cycles of Anxiety: How does anxiety sustain itself? Our framework models this using the R-dominant escapist regime (Figure 10D). Here, the interaction of rotational forces with error-amplifying gain produces a limit cycle—a self-sustaining loop that traps the subjective state in persistent rumination.

This reinterpretation provides a concrete bridge between dynamic theory and empirical observation. A key direction for future research is to formalize a mathematical transformation linking $G-\mu$ plane with the Valence–Arousal plane. Establishing this mapping would deepen our understanding of both the structure and dynamics of human emotion, creating a direct and testable interface between the two frameworks.

6. The Trinity Architecture: An Integrative Framework for FEP and PCT

6.1. An Architecture of Three Interacting Layers

To bridge the conceptual gap between the brain's physical basis and the mind's goal-directed nature, we propose the *Trinity Architecture*. This framework posits that our discrete computational model—the *Structural Layer* (SGBD)—functions as the crucial bridge between two other fundamental layers: the foundational *Physical Layer* (governed by FEP) and the goal-setting *Normative Layer* (governed by PCT).

- Layer 1: Physical Layer (FEP): The foundational layer representing the continuous physical basis of the mind.
- Layer 2: Structural Layer (SGBD): The intermediate layer describing the discrete computational model of subjectivity.
- Layer 3: Normative Layer (PCT): The highest layer, which functions as a hierarchical control system governing the entire architecture.

A detailed comparison of these layers is presented in Table 11. The dynamic cycle across them, illustrated in Figure 11, is best understood through an example: the process of overcoming a mental block.

- Layer 1 \rightarrow Layer 2 (Physical basis shapes computational structure): A physical state such as fatigue can alter the parameters of the computational model, for instance, by reducing affective gain G. This shallows the potential wells of the MTM, weakening concentration and diminishing task performance.
- Layer 2 \rightarrow Layer 3 (Structural state informs normative evaluation): The current state of the computational model, that is, the subjective state M_s , is evaluated by the hierarchical control system. A discrepancy from the normative goal (a PCT-like error) triggers a corrective response.
- Layer 3 \rightarrow Layer 2 (Parameter Modulation): Based on its evaluation, the normative layer modulates the parameters (G, μ) of the structural layer to guide the system toward its goals.
- Layer 3 \rightarrow Layer 1 (Implementation Lever): The normative layer can also employ meta-control strategies, using the implementation lever to act on the physical basis, for instance, by selecting an optimal style H or resetting the cognitive rhythm Δt to restore functional balance.

The dynamic interplay among the Physical, Structural, and Normative Layers, unfolding across distinct timescales, gives rise to adaptive and creative cognition. The agent orchestrating this complex interplay is the self-system S, whose computational mechanism we detail in the following section.

6.2. The Role of the Self-System S in The Trinity Architecture

As the core component of the *Normative Layer*, the self-system S is the agent responsible for driving the dynamic cycle across the architecture. We formalize S as a hierarchical Bayesian agent that learns and infers across two distinct timescales. This dual-timescale structure finds a powerful parallel in the distinction between the fast, intuitive System 1 and the slow, deliberate System 2 of dual-process theory (Kahneman, 2011), enabling both rapid adaptation and long-term personal development. Its mathematical formulation is provided in Subsection Appendix A.3.

- **Tactical Level (Fast Timescale):** On short timescales, the self-system acts as a tactical controller. It infers the optimal operational parameters (G, μ) based on the recent history of subjective states. This process generates the *Parameter Modulation* signals sent to the *Structural Layer*, corresponding to selecting the most suitable "tactic" for the present context.
- Strategic Level (Slow Timescale): On longer timescales, the self-system operates as a strategic learner. It updates its fundamental beliefs—the metaparameters θ_S that govern tactical inference—by evaluating the long-term outcomes of its actions against a core objective function, \mathcal{L} . This meta-learning process informs its meta-control strategies, such as when and how to use the *Implementation Lever* to act on the *Physical Layer*.

This hierarchical organization establishes a self-referential loop in which strategy θ_S guides tactics (G, μ) , and the outcomes of those tactics, evaluated against the objective function \mathcal{L} , in turn, drive the evolution of the strategy itself.

6.3. Contributions to Existing Theories

Within the proposed Trinity Architecture, the SGBD framework functions as the core "Structural Layer." This positioning allows it to serve not merely as a complementary model, but as a concrete *computational bridge* that integrates FEP and PCT. While both frameworks share the goal of "predicting or controlling perception," they are expressed in different formalisms: FEP as Bayesian inference (a generative model) and PCT as feedback control. The SGBD is proposed as the mechanism that mediates between the physical causality described by FEP and the teleological normativity of PCT. The following subsections detail how this Structural Layer contributes to the theories governing the other layers.

6.3.1. Contribution to the Free Energy Principle

Our framework provides a computational foundation, as the Structural Layer, for the principles of the Physical Layer described by FEP. In its adaptive regime (G > 0), our model's update rule can be interpreted

as a concrete, discrete-time implementation of the error-minimizing dynamics that FEP prescribes. The unique contribution of our model, however, lies in its ability to unify this healthy, FEP-compliant functioning with its potential collapse into pathology within a single formal structure. A crucial theoretical distinction must be emphasized. In FEP, the "precision" parameter is, by definition, non-negative. In contrast, our affective gain G can take negative values within the Structural Layer. This is not a mere technical difference; it is the defining feature that allows our model to formally capture the transition from FEP-like error minimization to the pathological, error-amplifying dynamics fundamental to a comprehensive theory of subjectivity. By allowing the gain to become negative (G < 0), the very same mechanism transitions from FEP-compliant dynamics to a pathological regime. This offers a formal account of the system's failure to minimize free energy, modeling pathology not as a special case, but as an emergent property of one coherent dynamical mechanism.

6.3.2. Contribution to Perceptual Control Theory

Our framework offers a computational substrate for the principles of PCT. We acknowledge that PCT originally proposes a detailed hierarchy of control, spanning from low-level intensity to high-level system concepts. The Trinity Architecture does not attempt to replicate this entire structure, but rather strategically models PCT's highest-level function—the goal-setting driven by principles and self-concept—as its Normative Layer. Our contribution is to provide a formal mathematical implementation of the Structural Layer (SGBD) that serves as the object of this top-down normative control. This approach allows us to formalize higher-order PCT concepts within the dynamics of the Structural Layer. For example, the rotational forces of Cognitive Phase Dynamics (CPD) offer a concrete mechanism for the "persistence" of hierarchical conflict, while the bifurcation structure of the Mind Topography Map (MTM) translates PCT's concept of "reorganization" into a specific mathematical event: a noise-induced transition to a new basin of attraction. The model thus provides a unified substrate that the Normative Layer governs, from which both elementary control and higher-order phenomena such as reorganization can naturally arise.

7. General Discussion

7.1. Summary of Theoretical Contributions

This paper makes six core theoretical contributions. To clarify their logical progression, we present them organized into three key themes:

Core Dynamics of the Scalar Model.

- 1. We introduced the MTM as a foundational "phase diagram" of subjectivity, demonstrating its isomorphism to a cusp catastrophe and establishing a formal basis for bistability, hysteresis, and the error-amplifying dynamics of psychopathology (G < 0).
- 2. We identified the IDE—a distinct zero-inertia state of pure responsiveness—and rendered it empirically testable via the indicator D_{IDE} , which quantifies the balance between cognitive "inertia" and "responsiveness."

Extension to Multidimensional Subjectivity.

- 3. We developed the multidimensional SGBD framework to move beyond a scalar representation of subjectivity, providing a formal "canvas" for modeling complex mental structures such as internal conflict.
- 4. We resolved the fundamental mechanistic duality of mental life by proposing CPD, a mechanism explaining how both stable "states" and persistent "processes" emerge from the symmetric and skew-symmetric components of the interaction matrix (\mathbf{W}_{Fe}), respectively. This mechanism was further operationalized through its empirical indicator D_{CPD} .

 $^{^8}$ If the objective function \mathcal{L} is interpreted as the Evidence Lower Bound (ELBO), this model connects naturally to the framework of FEP and active inference.

⁹See, for example, the comprehensive hierarchy detailed in Powers (1973).

Unifying Principles.

- 5. We established a methodological foundation by framing psychological stability as an "implementation problem," revealing that it critically depends on cognitive implementation styles H and temporal rhythms Δt .
- 6. We proposed the Trinity Architecture, an integrative framework that positions our model as a computational bridge mediating between the physical causality of the FEP and the teleological normativity of PCT.

7.2. Relation to Scientific Theories of Consciousness

Our model contributes to the scientific study of consciousness by offering a computational "engine" that integrates with other major theories, which are the focus of ongoing empirical investigation and debate (Melloni et al., 2023). As the following examples illustrate, our framework provides a dynamic mechanism for the static causal structures of IIT and a formal implementation of the "ignition" metaphor in GWT.

Dynamizing IIT's Causal Structures. The relationship with IIT, an ontological theory, is one of structure versus dynamics. IIT defines the static causal structure that constitutes an experience, whereas our framework provides the dynamic mechanism that operates *upon* that structure. If IIT offers the "hardware" blueprint of consciousness, our model supplies the "software" that runs on it, transforming IIT's causal snapshot into a dynamic movie of subjective experience.

Implementing GWT's Ignition Phenomenon. For GWT, a process-oriented theory, our framework provides a concrete mathematical implementation of its central metaphor of "ignition." GWT presents a functional account of conscious access, in which information must cross a nonlinear threshold to be globally "broadcast." Our model translates this functional description into a precise mathematical mechanism: the crossing of a bifurcation boundary on the MTM. This reframes ignition as a predictable, catastrophic transition, thereby offering a rigorous computational grounding for GWT's core claim.

7.3. Relation to the Philosophy of Mind: Functional Structuralism

Our framework's primary contribution to the philosophy of mind is an approach we term *Functional Structuralism*. This stance proposes to redefine the boundary between the "easy" and "hard" problems of consciousness (Chalmers, 1995). While the raw phenomenal quality of experience remains elusive, Functional Structuralism posits that the *structure* of subjective dynamics is mathematically tractable and thus falls within the domain of the "easy" problems.

The power of this approach is best illustrated by Cognitive Phase Dynamics (CPD). The phenomenological distinction between a stable psychological "state" and a dynamic "process"—a defining feature of inner experience—has long resisted formal description. Our model demonstrates that this distinction is not a philosophical enigma but corresponds directly to a fundamental mathematical property: the decomposition of the interaction matrix (\mathbf{W}_{Fe}) into its symmetric and skew-symmetric components.

By translating a core phenomenological feature into a formal mathematical property, this work embodies the promise of Functional Structuralism. It demonstrates that the architecture of inner experience possesses an analyzable structure, thereby taking a concrete step to extend the reach of scientific inquiry and bring a greater portion of the inner world within its grasp.

7.4. Limitations and Future Directions

As a broad theoretical framework, the primary limitations of this paper also define its most promising directions for future research. While additional constraints undoubtedly exist, the most significant ones fall into three categories—each stemming from deliberate strategic choices made to ensure conceptual clarity.

• Model Simplifications and Abstractions: To isolate the core mechanism of subjective dynamics, we deliberately assumed static parameters (G, μ) and adopted a canonical cubic saturation term. While this choice clarifies the model's essential structure, it necessarily omits the crucial process by which the self-system S dynamically learns and adapts these parameters over time.

- Methodological and Empirical Constraints: To first establish a coherent theoretical foundation, this paper has focused on the model's formal structure. As a result, the framework currently remains a theoretical construct awaiting direct empirical validation. A key challenge for future work is to develop robust estimation techniques that can fit the model's parameters to real-world psychological or neurocognitive data.
- Conceptual and Scope Limitations: To focus on the internal dynamics, this paper does not model the entire loop shown in Figure 1. Three key processes are omitted:
 - How external inputs are filtered by F_r to form M_o and then by F_i to influence M_s .
 - How the subjective state M_s generates an action A that influences the external world.
 - How feedback from the external world updates the self-system ${\cal S}.$

Completing this loop is a key direction for future work. Doing so would frame the internal dynamics analyzed herein as the core computational "engine" within a fully embodied agent.

Despite these limitations, the framework is not merely speculative. On the contrary, they directly give rise to a generative research program by making a set of falsifiable predictions that can be empirically tested to address these open challenges:

- Prediction 1 (Hysteresis Phenomenon): The model predicts that when system parameters enter the bistable region (G < 0), the dynamics will exhibit history dependence (hysteresis). This provides a directly testable model for clinically relevant phenomena such as mood relapse and belief perseverance.
- Prediction 2 (Dynamic Signature of IDE): As the system approaches the IDE state, its dynamic signature—quantified by the indicator D_{IDE} (indicator 1)—should converge toward zero. This hypothesis can be tested by manipulating task demands (affecting Δt) and measuring the resulting response dynamics.
- Prediction 3 (Pathological Process Signature): The transition from focused concentration to rumination should correspond to a measurable shift toward process-dominance, reflected in a decrease of the D_{CPD} indicator (indicator 2). This can be empirically tested by fitting a vector autoregressive (VAR) model to time-series data and computing D_{CPD} from the estimated interaction matrix.
- Prediction 4 (Adaptive Process Signature): Adaptive processes such as meditation—conceptualized as a pathway toward the IDE—should involve a controlled, temporary decrease in D_{CPD} . This transient shift into a process-dominant state facilitates escape from suboptimal attractors. Over the long term, practitioners should exhibit a baseline shift of their D_{IDE} indicator toward zero.
- Prediction 5 (Process Noise-Driven Reorganization): Increased process noise (σ) near the IDE should enhance response variance and increase the likelihood of a process noise-induced jump to a new stable state. This offers a mechanistic, testable account of PCT's concept of "reorganization."

8. Conclusion

To account for the phenomenological duality of subjectivity—its continuous flow and discrete transitions—this paper modeled the mind as a self-organizing discrete dynamical system within the Discrete-in-Continuous perspective. This approach revealed that psychological stability is implementation-dependent: identical continuous mechanisms may yield distinct discrete behaviors depending on cognitive style and temporal rhythm. From this foundation, the Mind Topography Map (MTM) was proposed as a formal phase diagram that captures catastrophic state shifts and the error-amplifying dynamics characteristic of psychopathology when G < 0.

Two complementary and dimensionless principles emerged from this framework. The *Ideal Dynamical Equilibrium* (IDE), quantified by $D_{\rm IDE}$, represents a zero-inertia state of pure responsiveness. The *Cognitive Phase Dynamics* (CPD), measured by $D_{\rm CPD}$, explains how the mind maintains both stable "states" and ongoing "processes" through the interplay of gradient and rotational dynamics. Together, these principles form the *Structural Layer* of the proposed *Trinity Architecture*, bridging the physical causality of the Free Energy Principle and the teleological normativity of Perceptual Control Theory.

By unifying these layers, the framework offers more than a theoretical synthesis—it provides a testable blueprint for computational psychiatry. Through the formal translation of phenomenological structure

into mathematical dynamics, it advances what we call *Functional Structuralism*: a program to render the architecture of the human mind a tractable object of scientific inquiry.

Call for Collaboration

The author is an independent researcher and welcomes opportunities for collaboration to further develop the framework presented in this paper, both theoretically and empirically. Comments, critiques, and suggestions for improvement are also warmly appreciated. Researchers interested in theoretical expansion, computational modeling, or empirical validation are encouraged to contact the author at:

takeoimaizumi@song.ocn.ne.jp (Takeo Imaizumi)

Declarations

Funding

No funding was received to support this research.

Conflict of Interest

The author declares that there are no conflicts of interest relevant to the content of this article.

Ethical Approval

Not applicable.

Data Availability

No datasets were generated or analyzed during the current study.

Code Availability

All Python code used to generate the figures (excluding conceptual diagrams) is available at: https://github.com/TakeoImaizumi/Python/

References

- Baars, B.J., 1988. A Cognitive Theory of Consciousness. Cambridge University Press.
- Chalmers, D.J., 1995. Facing up to the problem of consciousness. Journal of Consciousness Studies 2, 200–219.
- Dehaene, S., 2014. Consciousness and the Brain: Deciphering How the Brain Codes Our Thoughts. Viking.
- Dehaene, S., Changeux, J.P., 2011. Experimental and theoretical approaches to conscious processing. Neuron 70, 200–227. doi:10.1016/j.neuron.2011.03.018.
- Franklin, G.F., Powell, J.D., Workman, M.L., 1998. Digital Control of Dynamic Systems. 3rd ed., Addison-Wesley, Menlo Park, CA.
- Freeman, W.J., 2000. How Brains Make Up Their Minds. Columbia University Press, New York.
- Freud, S., 1923. The Ego and the Id. International Psycho-Analytical Press, Vienna. Translated by Joan Riviere.
- Friston, K., 2010. The free-energy principle: a unified brain theory? Nature Reviews Neuroscience 11, 127–138. doi:10.1038/nrn2787.
- van Gelder, T., 1995a. Dynamical hypotheses in cognitive science, in: Port, R.F., van Gelder, T. (Eds.), Mind as Motion: Explorations in the Dynamics of Cognition. MIT Press, Cambridge, MA, pp. 421–446.
- van Gelder, T., 1995b. What might cognition be, if not computation? The Journal of Philosophy 92, 345–381. doi:10.2307/2940963.
- Guckenheimer, J., Holmes, P., 1983. Nonlinear Oscillations, Dynamical Systems, and Bifurcations of Vector Fields. volume 42 of *Applied Mathematical Sciences*. Springer, New York. doi:10.1007/978-1-4612-1140-2.
- James, W., 1890. The Principles of Psychology. Henry Holt and Company, New York. doi:10.1037/11059-000.
- Kahneman, D., 2011. Thinking, Fast and Slow. Farrar, Straus and Giroux, New York.
- Kuznetsov, Y.A., 2004. Elements of Applied Bifurcation Theory. volume 112 of Applied Mathematical Sciences. 3rd ed., Springer, New York. doi:10.1007/b98848.
- Melloni, L., Mudrik, L., Pitts, M., Koyano, K.A., Gde, B.G., Tsuchiya, N., Koch, C., Tononi, G., Dehaene, S., Saad, Z.S., 2023. An adversarial collaboration to critically evaluate theories of consciousness. Nature Neuroscience 26, 1831–1843. doi:10.1038/s41593-023-01436-7.
- Powers, W.T., 1973. Behavior: The Control of Perception. Aldine, Chicago.
- Russell, J.A., 1980. A circumplex model of affect. Journal of Personality and Social Psychology 39, 1161–1178. doi:10.1037/h0077714.
- Strogatz, S.H., 2018. Nonlinear Dynamics and Chaos: With Applications to Physics, Biology, Chemistry, and Engineering. 2nd ed., CRC Press / Taylor & Francis, Boca Raton, FL. doi:10.1201/9780429492563.
- Tanaka, H.R., Krakauer, J.W., Sejnowski, T.J., 2019. The cognitive geometry of abstraction. Trends in Cognitive Sciences 23, 911–924. doi:10.1016/j.tics.2019.09.004.
- Tang, Y.Y., Hölzel, B.K., Posner, M.I., 2015. The neuroscience of mindfulness meditation. Nature Reviews Neuroscience 16, 213–225. doi:10.1038/nrn3916.

- Thom, R., 1975. Structural Stability and Morphogenesis: An Outline of a General Theory of Models. W. A. Benjamin, Reading, MA. Translated from the French by D. H. Fowler.
- Tononi, G., 2004. An information integration theory of consciousness. BMC Neuroscience 5, 42. doi:10. 1186/1471-2202-5-42.
- Zeeman, E.C., 1977. Catastrophe Theory: Selected Papers, 1972-1977. Addison-Wesley Publishing Company, Reading, MA.

Tables

Table 1: List of major symbols. This table offers a quick reference for the core mathematical notation used throughout the paper to build the dynamical model of subjectivity.

Symbol	Name	Description
M_s, M_s	Subjective state (scalar, vector)	The central variable of the model.
S	Self-system	The higher-order control system that modulates system parameters.
$G,oldsymbol{G}_{ ext{eff}}$	Affective gain (scalar, vector)	Sensitivity to the error signal.
$\mu,oldsymbol{\mu}_{ ext{eff}}$	Cognitive bias (scalar, vector)	The target point of the subjective state.
$\varepsilon(t), \pmb{\varepsilon}(t)$	Process noise (scalar, vector)	Transient random perturbations.
ω	Mental Fluctuation	The sum of internal perturbations ($\omega = \mu + \varepsilon$).
$oldsymbol{ heta}_S$	Metaparameters	The strategic-level parameters of the self-system $S.$
$\mathcal L$	Objective function	A function $\mathcal L$ that quantifies long-term goals.
IDE	Ideal Dynamical Equilibrium	A singular state of pure responsiveness where linear inertia vanishes.
$D_{ m IDE}$	IDE Indicator	A dimensionless metric for the balance between inertia and responsiveness.
D_{CPD}	CPD Indicator	A dimensionless metric for the balance between state and process dynamics.
$oldsymbol{g}_{ ext{input}},oldsymbol{\mu}_{ ext{input}}$	Source vectors	Universal inputs transformed by individual-specific structural matrices.
$\mathbf{M}_G,\mathbf{M}_{\mu}$	Structural matrices	Matrices that encode individual cognitive tendencies.
α, α	Saturation coefficient	The nonlinear stabilizing coefficient that prevents divergence.
$H, \Delta t$	Implementation	The method and time step for discretizing the continuous system.
Φ_H, Γ_H	Discretization coefficients	The inertia and drive coefficients dependent on the implementation.
\mathbf{W}_{Fe}	Interaction matrix	The evaluation weight matrix that defines the interactions among subjective dimensions.
\mathbf{S},\mathbf{R}	S/R components	The symmetric (S) and skew-symmetric (R) components of \mathbf{W}_{Fe} .

Table 2: Functional comparison of IDE and inertial states. This table contrasts the dynamic properties of the IDE state (G=1) with the disconnected inertial state (G=0), highlighting IDE as a state of adaptive, responsive equilibrium rather than mere inaction.

Feature	IDE $(G = 1, \mu = 0)$	Inertial State $(G=0, \mu=0)$
Stability Responsiveness Interpretation	Strongly stable Highly responsive to process noise Dynamic and adaptive equilibrium	Neutrally stable Unresponsive Static and disconnected state

Table 3: Mathematical comparison of discrete and continuous models. This table formally contrasts the properties of the discrete map used in this paper with its continuous-time origin. The comparison reveals that the discrete implementation uniquely gives rise to period-doubling (flip) bifurcations—a critical mechanism for modeling abrupt psychological shifts.

Item	Discrete Model (This Paper)	Continuous Model (Hypothesis)
State Update Rule	Difference Equation (Map) $M_{s,t+1} = (1-G)M_{s,t} - \alpha M_{s,t}^3 + G \mu + G \varepsilon(t)$	Differential Equation (Flow)
Deterministic Part	Map Function $f(M_s)$ $f(M_s) = (1 - G)M_s - \alpha M_s^3 + G \mu$	Drift Term $F(M_s)$ $F(M_s) = -GM_s - \alpha M_s^3 + G \mu$
Fixed-Point Condition	$M_{s,t+1} = M_{s,t}$ $\alpha (M_s^*)^3 + GM_s^* - G\mu = 0$	$\frac{\mathrm{d}M_s}{\mathrm{d}t} = 0$ $\alpha (M_s^*)^3 + GM_s^* - G\mu = 0$
Stability Condition	$ f'(M_s^*) < 1$ $(f'(M_s^*) = 1 - G - 3\alpha(M_s^*)^2)$	$F'(M_s^*) < 0$ $(F'(M_s^*) = -G - 3\alpha(M_s^*)^2)$
Nature of IDE $(G = 1, \mu = 0)$	Linear inertia vanishes. $M_{s,t+1} = -\alpha M_{s,t}^3 + \varepsilon(t)$	Strong linear restoring force. $dM_s = (-M_s - \alpha M_s^3) dt + \sigma dW_t$
Types of Bifurcation	Period-doubling (flip) Bifurcation: $f'(M_s^*) = -1$ \rightarrow Period-doubling, route to chaos	Hopf Bifurcation: (Does not occur in one-dimensional systems) \rightarrow Limit cycle

Table 4: Conceptual comparison of discrete and continuous systems. This table outlines the differing psychological interpretations of discrete versus continuous modeling. This comparison justifies our choice of a discrete framework to capture the "event-like" nature of subjective experience.

Comparison Item	Discrete Model (This Paper)	Continuous Model (Hypothesis)	
Affinity with Psychological Phenomena	Suitable for modeling "stepwise" or event- like phenomena such as decision-making, developmental stages, and learning trials.	Suitable for modeling "smooth" or "quantitative" phenomena such as changes in emotional intensity or mood waves.	
Nature of Attractors	Periodic points: Cycles through a finite number of points. Chaotic behavior can emerge even in one dimension (including in specific parameter regions of this model).	Limit cycles: Moves smoothly along a closed curve. Chaos occurs in three or more dimensions.	
Nature of IDE $(G = 1, \mu = 0)$	Dynamic and flexible responsiveness: The linear inertia term vanishes, directly reflecting process noise.	Responsive but strongly damped: A strong linear restoring force constantly pulls the state toward the center.	

Table 5: Effect of implementation style on discretization parameters. This table demonstrates how different discretization methods (implementation styles) alter the model's core coefficients, highlighting that the existence and conditions for IDE are implementation-dependent.

Style H	$\Phi_H(\kappa)$	$\Gamma_H(\kappa)$	IDE Condition
ZOH	$e^{-\kappa}$	$1 - e^{-\kappa}$	No finite solution for $\kappa > 0$;
			$\Phi_H \rightarrow 0$ as $\kappa \rightarrow \infty$
Tustin	$\frac{1-\kappa/2}{1+\kappa/2}$	$rac{\kappa}{1+\kappa/2}$	$\kappa=2 \ \Rightarrow \ \Phi_H=0, \ \Gamma_H=1$
forward Euler	$1 - \kappa^{'}$	κ	$\kappa = 1 \Rightarrow \Phi_H = 0, \ \Gamma_H = 1$
2nd-order Taylor	$1 - \kappa + \frac{\kappa^2}{2}$	$\kappa - rac{\kappa^2}{2}$	None

Table 6: Relationship between the discriminant and stability regions. This table explains how the sign of the discriminant of the fixed-point equation determines the number of real equilibria, which in turn defines the distinct regions of the Mind Topography Map.

Discriminant	Number of Real Roots	Region Type	Dynamic Behavior
$\tilde{\Delta} < 0$	1	Monostable / Unstable	The system has a single real equilibrium, which can be either stable or unstable depending on the gain G .
$\tilde{\Delta} > 0$	3	Bistable	The system has two stable equilibria, separated by an unstable one. The final state depends on initial conditions.
$\tilde{\Delta} = 0$	2 (one repeated)	Bifurcation Boundary	A qualitative change in the system's stability landscape occurs, separating the other regions.

Table 7: Four-quadrant classification on the G- μ plane. This table offers a heuristic for interpreting the Mind Topography Map by classifying the four quadrants based on the psychological meaning of the signs of gain G and bias μ .

Quadrant	Cognitive-Affective Label	Mathematical Basis (Discriminant & Stability)	Summary of Dynamic Features
$\overline{G > 0, \mu > 0}$	Adaptive Optimism	$\tilde{\Delta} < 0$. Contains both monostable and unstable regions.	Realistic enthusiasm. Flexible pursuit of goals.
$G<0, \mu>0$	Escapist Optimism	Sign of $\tilde{\Delta}$ depends on G, μ . monostable and bistable regions coexist.	Wishful thinking detached from reality. Amplifies beliefs.
$G<0,\mu<0$	Escapist Pessimism	Sign of $\tilde{\Delta}$ depends on G, μ . Monostable and bistable regions coexist.	Severe pessimism and helplessness. Fixation on a negative stable state.
$G>0, \mu<0$	Adaptive Vigilance	$\tilde{\Delta} < 0$. Contains both monostable and unstable regions.	Cautious realism. Predicts risks and deals with them constructively.

Table 8: Cross-disciplinary applications of Symmetric/Skew-symmetric decomposition. This table highlights the novelty of our psychological application by contrasting it with established uses in physics, engineering, and neuroscience. While the mathematical tool is common, its semantic mapping to psychological "states" and "processes" is the unique contribution of this paper.

Field	Object of Analysis	Symmetric (S) Interpretation	Skew-symmetric (R) Interpretation	Primary Goal
Physics / Mechanics	Force matrix, velocity gradient	Potential/conservative forces, strain/deformation	Non-potential/ rotational forces, vorticity	Analyze energy conservation, separate deformation from rotation.
Control Engineering	System state matrix \mathbf{A}	Rate of energy change (stability/instability)	Oscillatory behavior	Prove system stability, analyze transient response.
Computational Neuroscience (RNNs)	$\begin{array}{c} {\rm Recurrent} \\ {\rm weight\ matrix} \\ {\bf W}_{\rm rec} \end{array}$	Attractor dynamics (memory storage)	Sequential dynamics, temporal processing	Model memory and complex temporal computation.
This Paper (CPD)	Psychological interaction matrix \mathbf{W}_{Fe}	Stable psychological "states"	Persistent psychological "processes"	Explain the coexistence of states and processes in subjectivity.

Table 9: A 2x2 classification of the four psychodynamic regimes. The taxonomy is based on two axes: the sign of the affective gain G and the dominance of the symmetric (S) versus skew-symmetric (R) components of the evaluation matrix \mathbf{W}_{Fe} .

	G > 0 (Adaptive)	G < 0 (Escapist)
Symmetric (S-dominant)	Healthy Conflict / Mode Switching	Severe Internal Conflict / Dissociation
Skew-symmetric (\mathbf{R} -dominant)	Stable Rumination / Creative Process	Catastrophic Rumination / Vicious Cycle

Table 10: Parameter settings for the four most representative dynamic regimes. These parameters, assuming a zero cognitive bias ($\mu_{\rm eff}=0$), are chosen to most clearly illustrate the fundamental distinction between purely state-dominant (A, B) and process-dominant (C, D) dynamics, as shown in Figure 10.

Panel	G	D_{CPD}	\mathbf{W}_{Fe}	Comment
(A) Healthy Conflict	0.8	∞	$\begin{pmatrix} -1.0 & 0.0 \\ 0.0 & 1.0 \end{pmatrix}$	A symmetric system where the origin functions as a saddle point (choice point).
(B) Severe Conflict	-0.8	∞	$\begin{pmatrix} 1.0 & 0.0 \\ 0.0 & 1.0 \end{pmatrix}$	A symmetric system where stability is inverted by $G < 0$, making the origin a repeller.
(C) Stable Rumination	0.4	0.4	$\begin{pmatrix} 1.0 & 2.5 \\ -2.5 & 1.0 \end{pmatrix}$	A skew-symmetric system where attractive force (S) and rotational force (R) create a spiral convergence.
(D) Catastrophic Rumination	-0.4	0.4	$\begin{pmatrix} 1.0 & 2.5 \\ -2.5 & 1.0 \end{pmatrix}$	A skew-symmetric system where repulsive force $(G < 0)$ and rotational force (\mathbf{R}) create a spiral divergence.

Table 11: The three layers of the Trinity Architecture. This table summarizes the distinct roles and characteristics of each layer within the proposed integrative framework.

Layer	Core Description	Role and Timescale
Physical Layer (FEP)	Continuous Physical Basis	Provides the physical and informational grounding for the entire system. (Timescale: Fast, milliseconds to seconds)
Structural Layer (SGBD)	Discrete Computational Model	Implements the discrete dynamics of subjectivity, acting as the computational engine. (Timescale: Medium, seconds to minutes)
Normative Layer (PCT)	Hierarchical Control System	Governs the architecture through top-down modulation and meta-control to achieve goals. (Timescale: Slow, minutes to days)

Table 12: Situating the SGBD framework in relation to major theories of consciousness. This table is not intended as a competitive evaluation, but rather to clarify the unique contribution of the SGBD framework by highlighting its complementary role alongside IIT and GWT.

Comparison Item	IIT	GWT	SGBD Framework
Central Question	Ontology: What is the causal structure of experience? (Φ) .	Mechanism: How does conscious access occur? (Global broadcast & ignition). ^a	Implementation: How do discrete subjective dynamics emerge? (Bifurcation, IDE).
Concept of Time	Static (causal structure at a moment). ^b	Dynamic (ignition process over time).	Discrete-time dynamics (implementation-dependent stability).
Core Mechanism	Integrated information (Φ) , causal structure.	Global broadcast via network ignition. ^c	G- μ dynamics, IDE ($\Phi_H=0$), S/R decomposition.
Key Contribution	Provides a formal theory of what consciousness "is".	Provides a functional model of what consciousness "does".	Provides a computational model of how subjectivity "changes".
Treatment of Pathology	Outside of primary scope.	Explains failures of access (e.g., disorders of consciousness).	Models pathological dynamics via error-amplification $(G < 0)$.
Complementary Role	Provides the "hardware diagram" (static structure) for which SGBD could serve as the "software."	Provides the functional phenomenon (ignition) for which SGBD could serve as an implementation principle.	Complements IIT/GWT by offering a dynamic mechanism and bridging physics (FEP) with purpose (PCT).

^a (Baars, 1988; Dehaene and Changeux, 2011; Dehaene, 2014)

b IIT analyzes the causal structure of a system in a single state, which requires evaluating its potential past and future states, so "static" is a simplification for contrast.

^c This neuroan atomical substrate refers specifically to the Global Neuronal Work space (GNW) theory, a prominent version of GWT.

Table 13: A dynamic structural reinterpretation of NDDs. This table illustrates how the framework, particularly Cognitive Phase Dynamics (CPD), can offer a unifying language for generating hypotheses about the mechanisms underlying neurodevelopmental disorders.

Disorder	Example of Core Symptoms	A Potential Dynamic Structural Interpretation
Autism Spectrum Disorder (ASD) ^a	Restricted interests, cognitive rigidity, sensory hypersensitivity	A tendency toward State-Dominance (high D_{CPD}). Hypothesized as a system with overly stable, deep attractors, leading to fixation and difficulty in flexible state-switching.
Tic Disorders ^b	Sudden, involuntary movements or vocalizations	A tendency toward Process-Dominance (low $D_{\rm CPD}$). Involuntary actions approximated by limit cycle-like dynamics (processes) driven by strong rotational forces in motor-control circuits.
Attention- Deficit/Hyperactivity Disorder (ADHD) ^a	Inattention, hyperactivity, impulsivity, hyperfocus	Instability in Meta-Control. May involve instability in the meta-control of the state-process balance, leading to failures in both maintaining stable focus and disengaging from it.
Specific Learning Disorder (SLD)	Difficulties in specific academic skills	Could be associated with a localized distortion or vulnerability in the cognitive bias μ for a specific domain, creating a "hole" or "barrier" in the cognitive landscape.
Developmental Coordination Disorder (DCD)	Motor clumsiness, problems with coordination	Might be modeled as a challenge in the fine-tuning of affective gain G or response timing Δt within the sensory-motor control loop.

^a ADHD and ASD are presented as contrasting heuristics to illustrate the framework's potential. They are not intended as definitive clinical models.

^b The link between tics and "rotational dynamics" (process-dominance) is a core hypothesis derived from the framework's distinction between states and processes.

Figures

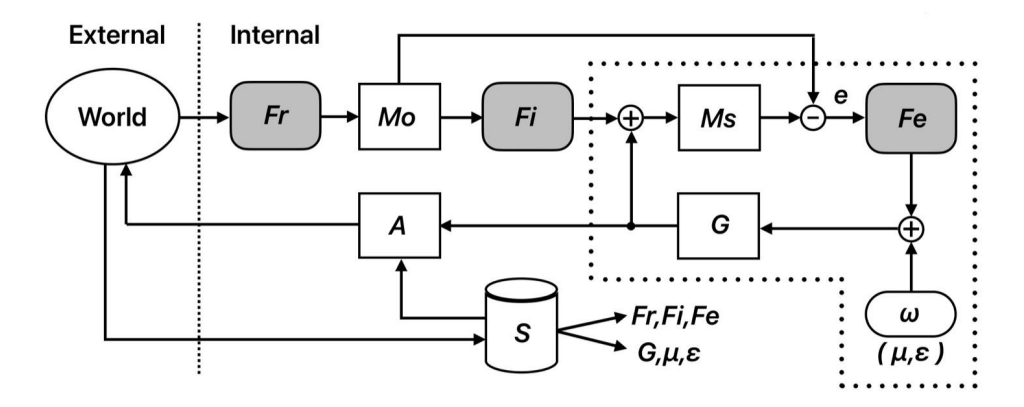


Figure 1: The control-theoretic blueprint for subjectivity. This conceptual diagram illustrates the information flow that generates subjective experience. External inputs are processed through recognition, interpretation, and evaluation filters, creating an error signal that drives the internal loop (dotted line). This internal loop is the focus of the mathematical formulation in Section 2.

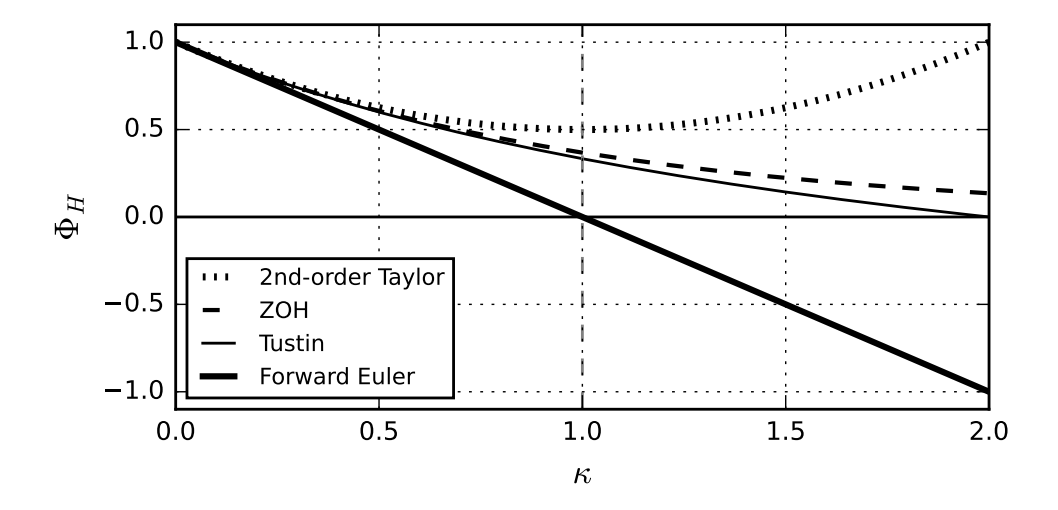


Figure 2: Implementation-dependent inertia. This figure illustrates how the system's inertia (memory of its past state) depends on the chosen implementation style H. The linear auto-regressive coefficient Φ_H is plotted against the dimensionless gain-timescale product κ . Each curve represents a different style; the zero-inertia IDE state occurs where a curve crosses the $\Phi_H = 0$ line. This demonstrates that core dynamic properties are shaped by cognitive styles or rhythms, a theme of Subsection 3.4.

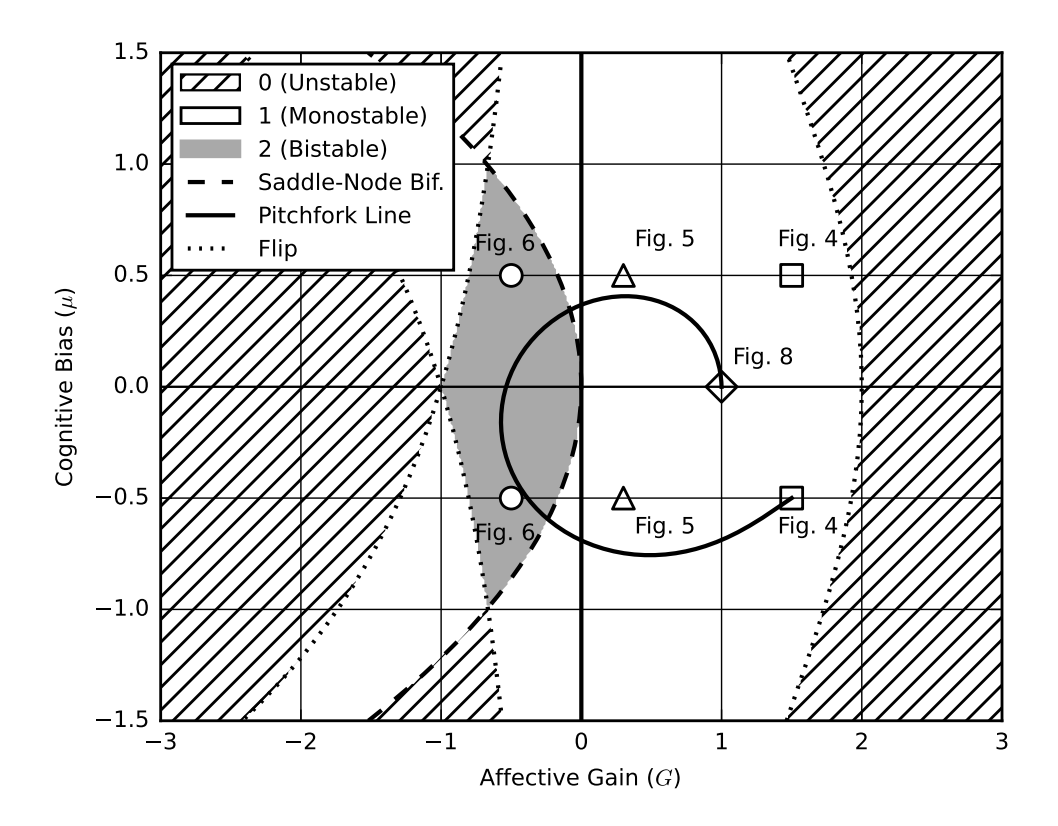


Figure 3: The Mind Topography Map (MTM). This figure visualizes the complete landscape of the model's stability as a function of affective gain G and cognitive bias μ . The plane is divided into regions by bifurcation boundaries, with shading indicating the number of stable states. This map serves as a "phase diagram" for subjectivity, allowing us to predict and interpret qualitative shifts in mental states as catastrophic jumps across boundaries. Markers show simulation points (Figures 4 to 8), and the spiral represents a navigated trajectory (Figure 9). On the $\mu=0$ axis, a flip bifurcation occurs at G=2 for the origin $(M_s=0)$ and at G=-1 for the non-zero fixed points (where $M_s\neq 0$).

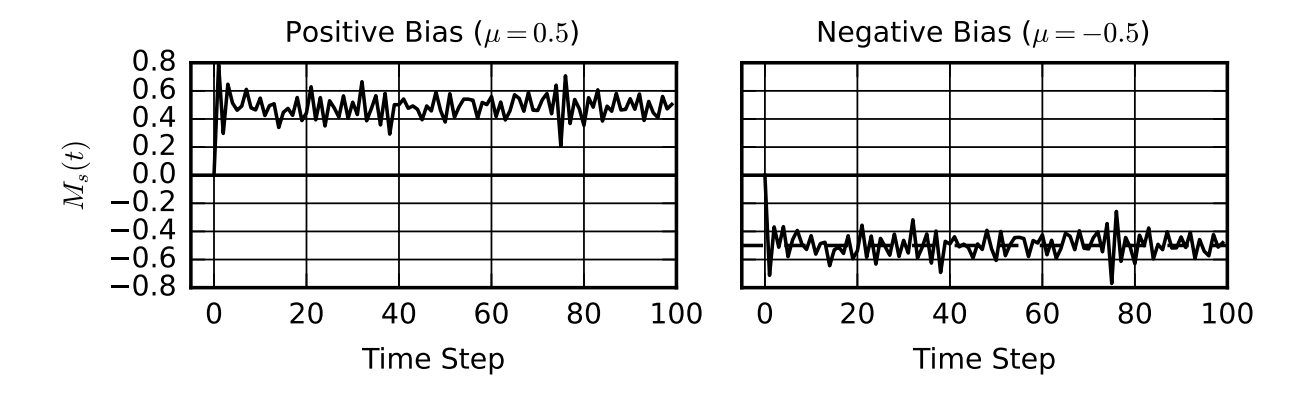


Figure 4: Representative dynamics: Adaptive, high-sensitivity region. Setting: $G=1.5, \mu=\pm0.5$. Behavior: The subjective state M_s converges rapidly and steeply to the target bias μ . Interpretation: This represents an overly sensitive or reactive response style, where the system strongly fixates on the goal.

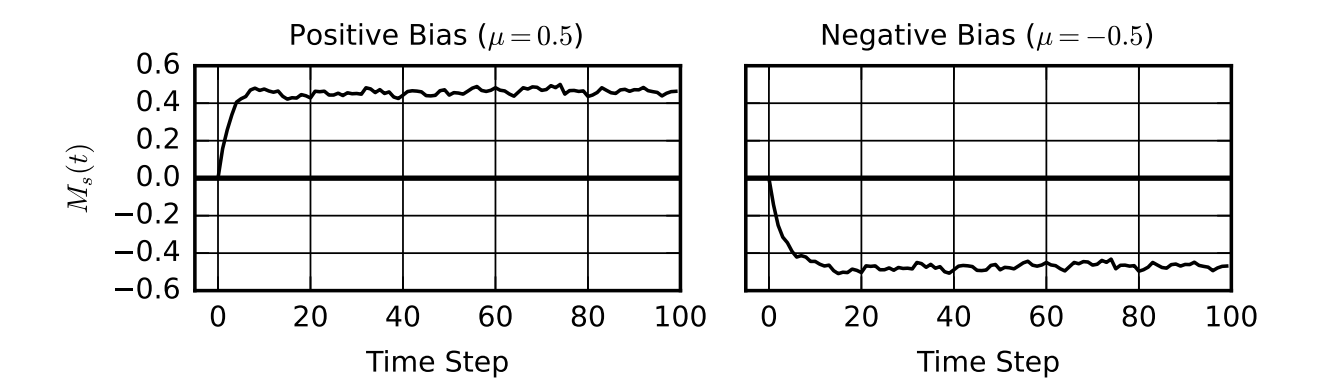


Figure 5: Representative dynamics: Adaptive, standard region. Setting: $G = 0.3, \mu = \pm 0.5$. Behavior: The subjective state M_s converges gradually to the target bias μ . Interpretation: This represents a moderate and stable response style, characteristic of a healthy adaptation or learning process.

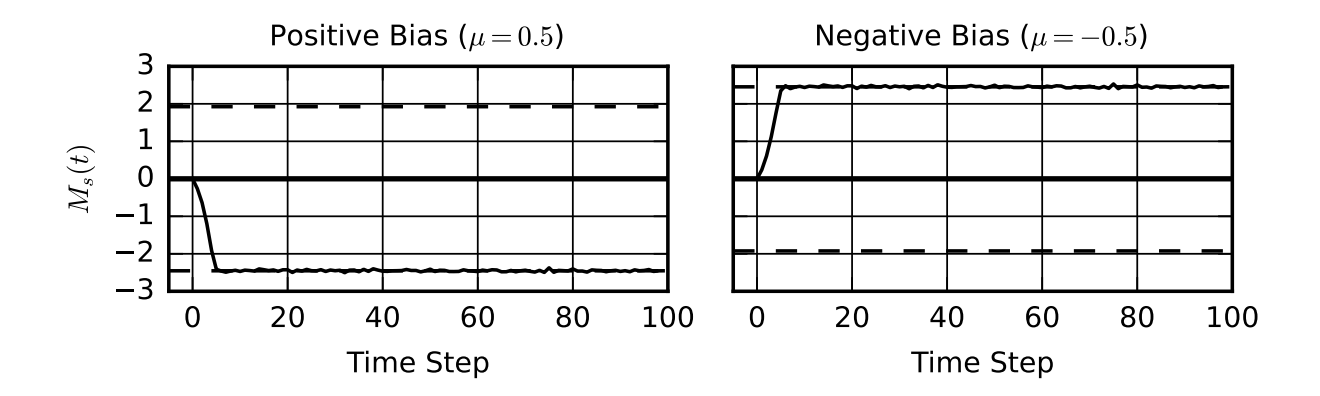


Figure 6: Belief amplification in the escapist, bistable region $(G < 0, \mu \neq 0)$. The subjective state M_s diverges from the small bias and, driven by process noise, settles into one of two distant attractors. This illustrates how a minor bias can be amplified into a strong conviction. The constant force from the $G\mu$ term breaks the symmetry of the attractors' locations and probabilities (see Figure 7).

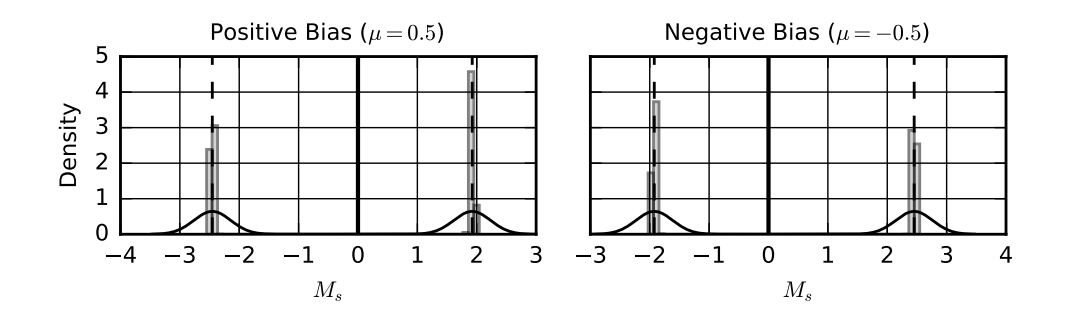


Figure 7: Statistical proof of bistability in the escapist region. The bimodal probability distribution confirms the existence of the two distinct attractors shown in Figure 6. The asymmetry in the attractors' height and position is caused by the cognitive bias μ , which tilts the potential landscape and makes the corresponding attractor more probable.

Method: The distribution was generated from two long simulations (N = 10,000 steps each), initiated from the vicinity of each stable attractor. The initial 1,000 transient steps of each run were discarded before combining the remaining data.

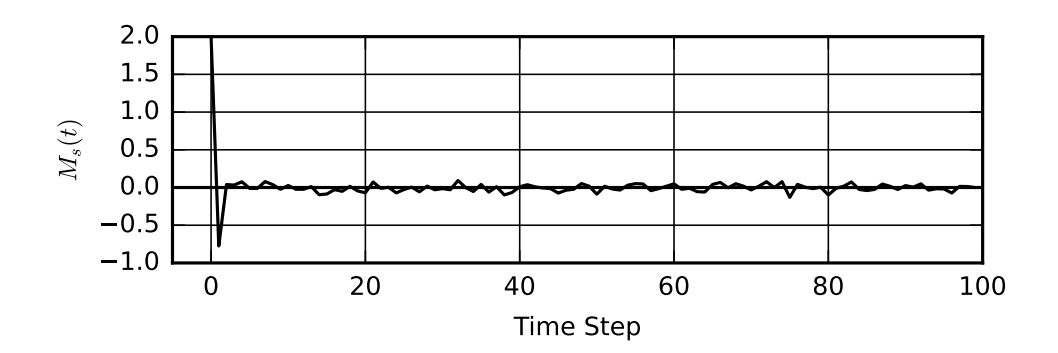


Figure 8: Representative dynamics: The IDE state. Setting: $G=1, \mu=0$. Behavior: With its linear inertia term gone, the subjective state M_s responds agilely to process noise without being attached to its past value, fluctuating around zero. Interpretation: This unique balance of responsiveness and stability makes IDE a key adaptive target for the self-system.

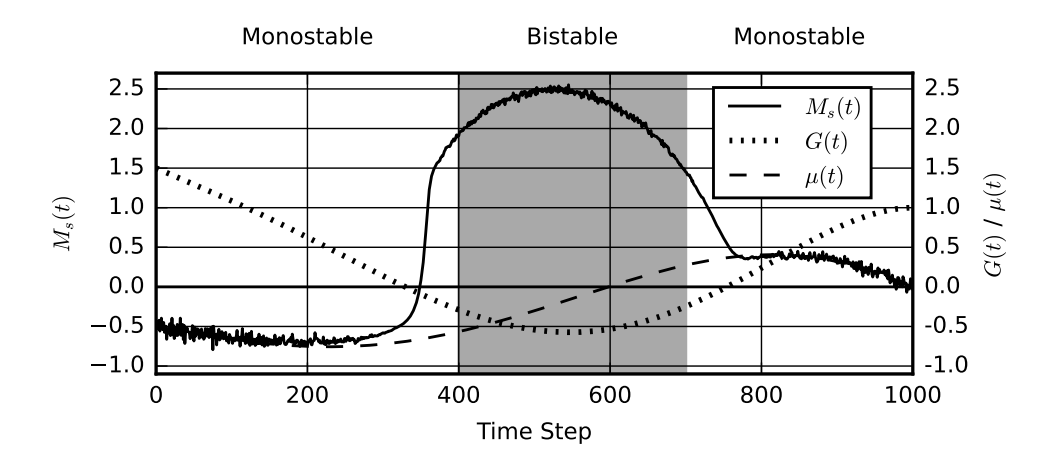


Figure 9: A proof of concept for dynamic self-regulation on the MTM. The subjective state $M_s(t)$ (solid line) responds to the self-system's active manipulation of gain G(t) (dotted) and bias $\mu(t)$ (dashed). The trajectory visualizes a complete mental journey: from adaptive tracking in the monostable region (Phase 1), through a catastrophic fixation within the bistable region (Phase 2), to a successful recovery in the monostable region and stabilization at the IDE (Phase 3).

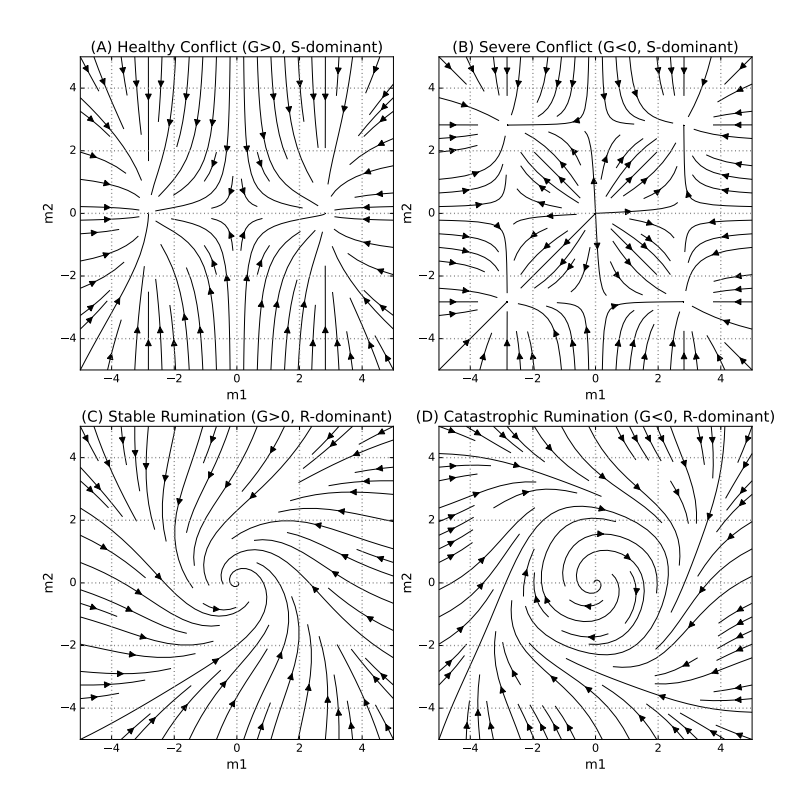


Figure 10: A taxonomy of the four most representative psychodynamic regimes. This figure illustrates the dynamics generated by the parameters in Table 10 (assuming $\mu_{\text{eff}} = 0$). (A) **Healthy Conflict** (G > 0, S-dominant): In a purely state-dominant system, adaptive gain creates a stable saddle point, modeling a clear choice. (B) **Severe Conflict** (G < 0, S-dominant): In a purely state-dominant system, escapist gain creates an unstable repulsion point, modeling a dissociative state. (C) **Stable Rumination** (G > 0, R-dominant): In a process-dominant system, adaptive gain creates a stable spiral convergence, modeling a thought process that finds a conclusion. (D) **Catastrophic Rumination** (G < 0, R-dominant): In a process-dominant system, escapist gain creates an unstable spiral divergence leading to a limit cycle, modeling a vicious cycle.

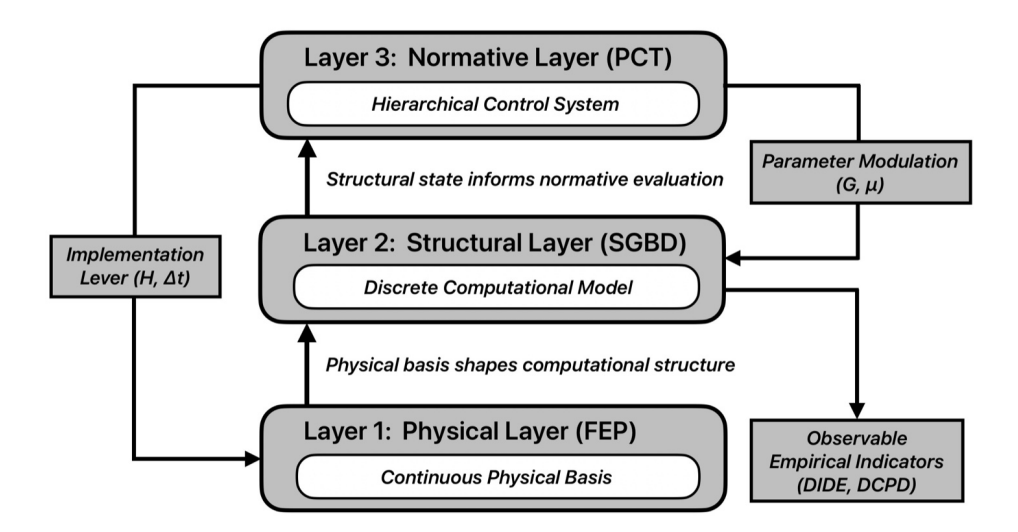


Figure 11: The Trinity Architecture. This diagram illustrates the proposed integrative framework. It posits three interacting layers: a foundational *Physical Layer* (FEP) representing the continuous physical basis, an intermediate *Structural Layer* (SGBD) implementing a discrete computational model, and a top-level *Normative Layer* (PCT) functioning as a hierarchical control system. The arrows depict the dynamic cycles of influence, modulation, and control that link the layers.

Appendices

Appendix A. Mathematical Foundations of the Model

Appendix A.1. The Core Scalar Model

Appendix A.1.1. Implementation Styles and Eigenvalue Mapping

The relationship between implementation styles and dynamics, as presented in Section 3, follows standard methods used in control engineering for discretizing continuous systems. The derivations for the main cases are outlined below, beginning with the simple linear continuous system $\frac{dM_s(t)}{dt} = \lambda_c M_s(t)$, whose discrete counterpart is $M_{s,t+1} = \lambda_d M_{s,t}$.

- 1. Zero-Order Hold (ZOH). This method provides an exact discretization under the assumption that the input remains constant between steps. The exact solution of the continuous system, $M_s((t+1)\Delta t) = e^{\lambda_c \Delta t} M_s(t\Delta t)$, perfectly matches the form of the discrete system. Thus, direct comparison yields $\lambda_d = e^{\lambda_c \Delta t}$.
- 2. Forward Euler Method. This is the simplest first-order approximation based on the definition of a derivative. Approximating the continuous differential equation using a forward difference gives $\frac{M_{s,t+1}-M_{s,t}}{\Delta t} \approx \lambda_c M_{s,t}$. Solving for $M_{s,t+1}$ yields $M_{s,t+1} = (1 + \lambda_c \Delta t) M_{s,t}$, from which $\lambda_d = 1 + \lambda_c \Delta t$. For the forward Euler method, stability requires $|\lambda_d| < 1 \Leftrightarrow -2 < \lambda_c \Delta t < 0$.
- 3. Tustin's Method (Bilinear Transform). This method offers a more accurate approximation based on the trapezoidal rule. Integrating the continuous differential equation and approximating the integral using

the trapezoidal rule gives $M_{s,t+1}-M_{s,t}\approx \frac{\Delta t}{2}(\lambda_c M_{s,t}+\lambda_c M_{s,t+1})$. Solving for $M_{s,t+1}$ yields $M_{s,t+1}=\frac{1+\lambda_c\Delta t/2}{1-\lambda_c\Delta t/2}M_{s,t}$, from which we obtain $\lambda_d=\frac{1+\lambda_c\Delta t/2}{1-\lambda_c\Delta t/2}$. For a system that includes an input μ , the trapezoidal approximation leads to the discrete update form $M_{s,t+1}=\Phi_H M_{s,t}+\Gamma_H \mu_t$, where $\Phi_H=\frac{1-\frac{G\Delta t}{2}}{1+\frac{G\Delta t}{2}}$ and $\Gamma_H=\frac{G\Delta t}{1+\frac{G\Delta t}{2}}$. The input gain for Tustin's method increases monotonically for $\kappa>0$, with $\lim_{\kappa\to\infty}\Gamma_H=2$.

Identification of Discrete Process Noise Covariance. To ensure a fair comparison between different implementation styles (H), the covariance Q_H of the discrete process noise must be defined so as to preserve the statistical properties of the underlying continuous system. We achieve this by matching the stationary variance of the discrete linear system with that of the continuous one. The stationary variance of the linear part of the continuous system Equation (2) is $Var_{\infty} = \frac{G\sigma^2}{2}$, whereas for the discrete linear system $M_{k+1} = \Phi_H M_k + w_k$, it is $Var_{\infty} = \frac{Q_H}{1-\Phi_H^2}$. Equating these two gives the following definition of Q_H , under the assumption of stability $(G > 0 \text{ and } |\overset{\circ}{\Phi}_H(G, \Delta t)| < 1)$:

$$Q_H = \frac{G\sigma^2}{2}(1 - \Phi_H(G, \Delta t)^2)$$
 (Appendix A.1)

This ensures that all comparisons between implementation styles in this paper are rigorous.

The diffusion intensity in the continuous system depends on $(G\sigma)^2$, so the sign of G does not directly affect the width of the distribution, although it does affect the mean dynamics. For $\alpha > 0$, this one-dimensional diffusion process has an invariant distribution $p_*(x) \propto \exp[-2V(x)/(G\sigma)^2]$, where the potential is given by $V(x) = \frac{G}{2}x^2 + \frac{\alpha}{4}x^4 - G\mu x.$

As discussed in Section 7, these process noise-induced fluctuations act as the driving force that enables the system to escape maladaptive stable states and explore new possibilities.

Appendix A.1.2. Bifurcation and Stability Analysis

The qualitative behavior of the system is revealed by analyzing the deterministic part of Equation (4), $f(M_s) = (1 - G\Delta t)M_s - \alpha \Delta t M_s^3 + G\Delta t \mu$. The following analysis assumes $\Delta t = 1$.

Fixed Points and Potential Function. This discrete map can be interpreted as approximately "gradient-like," such that $f(M_s) - M_s = -\partial_{M_s} V(M_s)$. In this case, since $V'(M_s) = M_s - f(M_s) = GM_s + \alpha M_s^3 - G\mu$, the potential function is:

 $V(M_s) = \frac{G}{2}M_s^2 + \frac{\alpha}{4}M_s^4 - G\mu M_s.$ (Appendix A.2)

This interpretation is an approximation valid for reasonably small Δt ; it does not imply that a strict Lyapunov function always exists for a general one-dimensional map. A fixed point M_s^* satisfies $f(M_s^*) = M_s^*$, as given in Equation (3).

Linear Stability Analysis. The stability of a fixed point M_s^* is determined by the derivative (Jacobian) of $f(M_s)$ at that point: $f'(M_s^*) = (1 - G) - 3\alpha(M_s^*)^2$. The condition for stability is $|f'(M_s^*)| < 1$.

Derivation of Bifurcation Boundaries. Bifurcations occur at points where the stability condition is violated, i.e., when $|f'(M_s^*)| = 1$.

Saddle-Node Bifurcation ($f'(M_s^*) = 1$): This condition implies $-G = 3\alpha(M_s^*)^2$. Solving this simultaneously with the fixed-point equation to eliminate M_s^* yields the curve on the $G-\mu$ plane where a saddle-node bifurcation occurs:

 $G = -\frac{27\alpha}{4}\mu^2. (Appendix A.3)$

Period-Doubling (Flip) Bifurcation ($f'(M_s^*) = -1$ **):** This condition implies $2 - G = 3\alpha(M_s^*)^2$. Eliminating M_s^* from this equation and the fixed-point equation gives the curve along which a period-doubling (flip) bifurcation occurs:

$$\mu^2 = \frac{4(1+G)^2(2-G)}{27\alpha G^2}.$$
 (Appendix A.4)

This equation is valid for $G \neq 0$ and $2 - G \geq 0$ (i.e., $G \leq 2$). Notably, along the symmetry axis $\mu = 0$, the critical point is G = 2, since f'(0) = 1 - G; period-doubling begins here for the fixed point at the origin. Moreover, for the non-zero fixed points that exist when G < 0, a flip bifurcation occurs at G = -1.

Symmetric Bifurcation: Under the symmetry condition $\mu = 0$, a pitchfork-type bifurcation occurs at G = 0, where the fixed points $\pm \sqrt{-G/\alpha}$ emerge.

These equations collectively define the boundaries of the stability regions depicted in the Mind Topography Map (Figure 3).

Appendix A.2. The Multidimensional SGBD Framework

The mathematical foundation of the Structural Gain–Bias Dynamics (SGBD) framework, outlined in Section 5, is detailed below.

Appendix A.2.1. Derivation of the Multidimensional Update Rule

The update of the subjective state vector $M_s(t) \in \mathbb{R}^N$ in the SGBD framework consists of the following components:

- 1. An inertia term representing the current state: $M_s(t)$
- 2. A nonlinear saturation term preventing divergence: $-\alpha \odot (M_s(t))^{\circ 3}$
- 3. An update signal: UpdateSignal(t)

The update signal integrates internal and external influences and scales them by the affective gain. The evaluation filter (Fe) first processes the error $\boldsymbol{E}(t) = \boldsymbol{M_o}(t) - \boldsymbol{M_s}(t)$ between the objective state $\boldsymbol{M_o}$ and the subjective state $\boldsymbol{M_s}$. Under the simplification in the main text ($\boldsymbol{M_o} = 0$), this becomes $\boldsymbol{E}(t) = -\boldsymbol{M_s}(t)$. The processing by Fe is modeled as a linear transformation:

$$\boldsymbol{E}_{\text{eval}}(t) = -\mathbf{W}_{\text{Fe}}(S, t)\boldsymbol{M}_{\!s}(t),$$

where \mathbf{W}_{Fe} is the evaluation weight matrix. The effective bias $\boldsymbol{\mu}_{\text{eff}}(t)$ and process noise $\boldsymbol{\varepsilon}(t)$ are added to this evaluated error to form the core of the update signal. The entire signal is then scaled elementwise by the effective gain vector $\boldsymbol{G}_{\text{eff}}(t)$.

Integrating these components yields the general update equation:

$$M_s(t+1) = M_s(t) - \alpha \odot (M_s(t))^{3} + G_{\text{eff}}(t) \odot (-W_{\text{Fe}}M_s(t) + \mu_{\text{eff}}(t) + \varepsilon(t)).$$
 (Appendix A.5)

A core hypothesis of the framework is that these effective vectors, G_{eff} and μ_{eff} , are generated by individual-specific structural matrices, \mathbf{M}_G and \mathbf{M}_{μ} , which transform universal source vectors, $\mathbf{g}_{\text{input}}$ and $\boldsymbol{\mu}_{\text{input}}$:

$$G_{\text{eff}}(t) = \mathbf{M}_G g_{\text{input}}(t),$$
 (Appendix A.6)

$$\mu_{\text{eff}}(t) = \mathbf{M}_{\mu} \mu_{\text{input}}(t).$$
 (Appendix A.7)

In this formulation, the source vectors can be conceptualized as representing universal psychological inputs, such as general arousal or valence. The structural matrices, in contrast, function as personalized "cognitive wiring diagrams," encoding an individual's unique emotional and cognitive tendencies. This provides a powerful mechanism for modeling individual differences. In the simplest case, where the structural matrices are identity matrices (\mathbf{I}) , the effective vectors equal the source vectors.

Appendix A.2.2. Decomposition of \mathbf{W}_{Fe} and Properties of the Dynamical System

The properties of \mathbf{W}_{Fe} fundamentally determine the system's dynamics. Any matrix can be uniquely decomposed into the sum of a symmetric component (S) and a skew-symmetric component (R): $\mathbf{W}_{\mathrm{Fe}} = \mathbf{S} + \mathbf{R}$.

Symmetric component $\mathbf{S} = \frac{1}{2}(\mathbf{W}_{Fe} + \mathbf{W}_{Fe}^{\top})$ and gradient dynamics. This component gives rise to the system's gradient dynamics. The deterministic update vector (without process noise) can be expressed as the negative gradient $-\nabla V$ of a potential function $V(\mathbf{M}_s)$. To clarify correspondence with the discussion in the main text, if \mathbf{G}_{eff} is represented by a scalar G for simplicity, the potential function is:

$$V(\mathbf{M}_s) = \frac{1}{2} \mathbf{M}_s^{\top} \mathbf{S} \mathbf{M}_s + \frac{1}{4} \sum_{i=1}^{N} \alpha_i M_{s,i}^4 - G \boldsymbol{\mu}^{\top} \mathbf{M}_s + \dots$$
 (Appendix A.8)

The behavior of a gradient system converges to fixed points—the stable valleys (local minima) of this potential landscape—corresponding to psychologically static, equilibrium states.

Skew-symmetric component $\mathbf{R} = \frac{1}{2}(\mathbf{W}_{Fe} - \mathbf{W}_{Fe}^{\top})$ and rotational dynamics. The skew-symmetric component generates rotational forces that do not alter the potential (since for any vector \mathbf{v} , $\mathbf{v}^{\top}\mathbf{R}\mathbf{v} = 0$). This force causes the state to orbit on the potential landscape, producing dynamic behaviors that cannot arise from gradient forces alone.

Appendix A.2.3. Dynamic Attractors and the Neimark-Sacker Bifurcation

The stability of the system is determined by the eigenvalues of the Jacobian matrix J of the update function at a fixed point M_s^* . The fixed point is stable if all eigenvalues satisfy $|\lambda_i| < 1$.

When \mathbf{W}_{Fe} includes a skew-symmetric component (i.e., is asymmetric), the Jacobian J can have complex conjugate eigenvalues. As parameters vary, if the magnitude of a complex-conjugate pair exceeds one, the fixed point loses stability, and a stable limit cycle (an invariant closed curve) emerges around it. This phenomenon is known as a Neimark–Sacker bifurcation, a primary mechanism by which discrete dynamical systems produce sustained oscillations (psychological processes).

This mathematical mechanism provides the theoretical basis for why the SGBD framework can coherently describe not only static psychological states but also dynamic processes such as rumination.

Appendix A.2.4. Derivation of the Vectorized IDE State

Within the SGBD framework, there exists a unique equilibrium corresponding to the Ideal Dynamical Equilibrium (IDE) state in the scalar model. Its derivation proceeds by analogy with the simplified scalar equation (4) using the forward Euler method. Assuming $\mathbf{W}_{\mathrm{Fe}} = \mathbf{I}$ (the identity matrix), the update rule becomes:

$$M_s(t+1) = M_s(t) - \alpha \odot (M_s(t))^{\circ 3} + G_{\text{eff}}(t) \odot (-M_s(t) + \mu_{\text{eff}}(t) + \varepsilon(t)).$$

Rearranging gives a structure analogous to the scalar model's equation (4):

$$M_{\rm s}(t+1) = (\mathbf{1} - G_{\rm eff}(t)) \odot M_{\rm s}(t) - \boldsymbol{\alpha} \odot (M_{\rm s}(t))^{\circ 3} + G_{\rm eff}(t) \odot \boldsymbol{\mu}_{\rm eff}(t) + G_{\rm eff}(t) \odot \boldsymbol{\varepsilon}(t),$$

where $\mathbf{1}$ is a vector of ones. Just as the IDE state in the scalar model arises when the inertia term (1-G) vanishes at G=1, the vectorized IDE state corresponds to $(\mathbf{1}-\boldsymbol{G}_{\text{eff}}(t))$ becoming a zero vector when $\boldsymbol{G}_{\text{eff}}(t)=\mathbf{1}$.

Substituting the IDE conditions, $G_{\text{eff}}(t) = 1$ and $\mu_{\text{eff}}(t) = 0$, yields:

$$M_s(t+1) = (\mathbf{1} - \mathbf{1}) \odot M_s(t) - \boldsymbol{\alpha} \odot (M_s(t))^{\circ 3} + \mathbf{1} \odot \mathbf{0} + \mathbf{1} \odot \boldsymbol{\varepsilon}(t)$$
$$= -\boldsymbol{\alpha} \odot (M_s(t))^{\circ 3} + \boldsymbol{\varepsilon}(t).$$

This is the direct vector extension of the scalar IDE equation $M_{s,t+1} = -\alpha M_{s,t}^3 + \varepsilon(t)$. It describes a dynamic yet balanced equilibrium in which each subjective dimension is freed from its linear autoregressive term (inertia) and driven solely by the instantaneous process noise and the nonlinear stabilizing term.

Appendix A.3. A Bayesian Model of the Self-System S

This section provides a detailed mathematical formulation of the self-system S, as outlined in Subsection 6.2, from the perspective of hierarchical Bayesian learning.

Appendix A.3.1. Tactical Control (Fast Timescale)

On a fast timescale, the self-system S determines the optimal operational parameters (G, μ) through Bayesian inference, based on the observed history of subjective states $\{M_s\}_{hist}$ and the current context (objective model M_o). This can be expressed as maximizing the following posterior probability:

$$P(G, \mu \mid \{M_s\}_{hist}, M_o, \theta_S) \propto P(\{M_s\}_{hist} \mid G, \mu, M_o) P(G, \mu \mid \theta_S)$$
 (Appendix A.9)

Here, $P(\{M_s\}_{hist} \mid \dots)$ represents the likelihood—how well a specific set of (G, μ) explains the observed state history—while $P(G, \mu \mid \theta_S)$ denotes the prior, reflecting the current control policies and beliefs of the self-system S, as defined by the metaparameters θ_S . The self-system regulates subjective dynamics by selecting, for example, the pair (G^*, μ^*) that maximizes this posterior (MAP estimation). In the multidimensional SGBD framework, the likelihood can be written as:

$$oldsymbol{M}_{s,t+1}\!\sim\!\mathcal{N}\!\!\left(\Phi_{H}oldsymbol{M}_{s,t}-oldsymbol{lpha}\!\odot\!oldsymbol{M}_{s,t}^{\circ3}+\Gamma_{H}oldsymbol{\mu},\,oldsymbol{Q}_{H}
ight)\!,$$

where Q_H is the multidimensional process noise covariance (see Subsubsection Appendix A.1.1), assumed to have a diagonal or low-rank structure under the conditions G > 0 and $|\Phi_H| < 1$.

Appendix A.3.2. Strategic Learning (Slow Timescale)

On a slower timescale, the self-system S learns its own control policies—the metaparameters θ_S —through meta-learning. This process evaluates the trajectory of subjective states $\{M_s\}_{\text{traj}}$, generated under tactical-level control, using a long-term objective function \mathcal{L} . The update rule for θ_S follows a general stochastic gradient ascent:

$$\boldsymbol{\theta}_{S}^{(k+1)} = \boldsymbol{\theta}_{S}^{(k)} + \eta_{\theta} \nabla_{\boldsymbol{\theta}_{S}} \mathbb{E}[\mathcal{L}(\{M_{s}\}_{\text{traj}}, M_{o} \mid \boldsymbol{\theta}_{S}^{(k)})], \tag{Appendix A.10}$$

where k is the learning epoch and η_{θ} is the meta-learning rate. The objective function \mathcal{L} can reflect various goals depending on context—for instance, (a) maximizing model evidence (ELBO maximization) or (b) maintaining proximity to IDE or minimizing an error cost.

The operational parameters themselves may evolve as slow stochastic processes with small process noise satisfying $\varepsilon_{\{\cdot\}} \ll 1$, ensuring a clear timescale separation between the fast Bayesian update (tactical level) and the slow variation of priors (strategic level):

$$G_{t+1} = G_t + \varepsilon_G \eta_t, \quad \mu_{t+1} = \mu_t + \varepsilon_\mu \zeta_t.$$

Appendix A.3.3. Implementation and Inference

Identifiability and Regularization.. With limited observational data, care must be taken regarding the identifiability of parameters G and μ , as the mean drift term depends on the product $G\mu$ and the variance on $(G\sigma)^2$. This issue can be mitigated through: (i) experimental manipulations, such as varying the thinking time (Δt) or introducing external perturbations (temporary shifts in μ); and (ii) weak regularization of the prior distributions p(G), $p(\mu)$, e.g., $G \sim \mathcal{N}(1, \tau_G^2)$, $\mu \sim \mathcal{N}(0, \tau_\mu^2)$.

Inference Methods. Several computational methods are applicable for online parameter inference. For the scalar model, extended Kalman filters or particle filters are effective. For higher-dimensional cases in the SGBD framework, more powerful approximate inference techniques such as Variational Bayes (VB–EM) or Stochastic Gradient Variational Inference (SGVI) are required.

Algorithm Overview. This hierarchical learning process is summarized in the pseudocode shown in Algorithm 1.

Algorithm 1 Hierarchical Bayesian Learning and Control of the Self-System S

```
1: Input: Metaparameters \boldsymbol{\theta}_{S}^{(k)}
    procedure REGULATEANDLEARNCYCLE
          Tactical Level (fast timescale)
          for t = 1 to T do
 3:
               Observe subjective state history \{M_s\}_{hist} and context M_o
 4:
               Construct prior P(\boldsymbol{G}, \boldsymbol{\mu} \mid \boldsymbol{\theta}_{S}^{(k)})
 5:
               Compute likelihood P(\{M_s\}_{\text{hist}} \mid \boldsymbol{G}, \boldsymbol{\mu}, M_o)
 6:
               Evaluate posterior P(G, \mu \mid ...) and select (G^*, \mu^*) (e.g., MAP estimation)
 7:
               Update subjective dynamics using (G^*, \mu^*) and record trajectory \{M_s\}_{\text{traj}}
 8:
          end for
 9:
         Strategic Level (slow timescale)
          Evaluate \mathbb{E}[\mathcal{L}] based on the collected trajectory
10:
          Update metaparameters: \boldsymbol{\theta}_{S}^{(k+1)} \leftarrow \boldsymbol{\theta}_{S}^{(k)} + \eta_{\theta} \nabla_{\boldsymbol{\theta}_{S}} \mathbb{E}[\mathcal{L}]
11:
12: end procedure
```

Appendix B. Connection to Cusp Catastrophe Theory

This appendix connects our framework with the seminal ideas of catastrophe theory (Thom, 1975), a framework that has had a profound influence on theoretical psychology (Zeeman, 1977). We demonstrate that the bifurcation structure of the Mind Topography Map (MTM) is mathematically isomorphic to the canonical form of a cusp catastrophe, as shown below.

The potential function V(x) of a cusp catastrophe is defined by the canonical form:

$$V(x; a, b) = \frac{1}{4}x^4 + \frac{1}{2}ax^2 + bx,$$
 (Appendix B.1)

where x is the state variable and a and b are the control parameters. The equilibrium states of the system are determined by the stationary points of this potential, obtained by setting its gradient to zero:

$$\frac{\partial V}{\partial x} = 0 \quad \Rightarrow \quad x^3 + ax + b = 0.$$
 (Appendix B.2)

In our model, the fixed-point equation (see Equation (3)) is given by:

$$\alpha (M_s^*)^3 + GM_s^* - G\mu = 0.$$
 (Appendix B.3)

Dividing both sides by α (with $\alpha > 0$) yields a form directly corresponding to the canonical cusp equation:

$$(M_s^*)^3 + \left(\frac{G}{\alpha}\right)M_s^* + \left(-\frac{G\mu}{\alpha}\right) = 0.$$
 (Appendix B.4)

Comparison with Equation (Appendix B.2) reveals the following variable correspondence:

- State variable: $x \leftrightarrow M_s^*$
- Control parameters: $a \leftrightarrow G/\alpha$, $b \leftrightarrow -G\mu/\alpha$

This mathematical isomorphism is significant: it confirms that the MTM is not merely a conceptual visualization but a concrete instantiation of the canonical structure predicted by catastrophe theory.

Our deliberate choice of the cusp catastrophe (codimension 2) is both minimal and necessary. It is the simplest form capable of capturing the interaction between the two fundamental control parameters of our model—affective gain G and cognitive bias μ . A fold catastrophe (codimension 1) would be insufficient, as it includes only one control parameter, whereas higher-order forms such as the butterfly catastrophe (codimension 4) would introduce superfluous complexity for our aim of defining the basic generative mechanism of subjectivity.

At the same time, this focused formulation opens a clear path for future extensions. Modeling the richer mental structures described within the SGBD framework may require the explanatory reach of higher-order catastrophes. Thus, the present analysis provides a robust mathematical cornerstone—grounding our model in a canonical formalism while laying a principled foundation for future theoretical development.

Appendix C. Conceptual Application to Neurodevelopmental Disorders (NDDs)

Appendix C.1. Purpose and Positioning

This appendix presents a conceptual extension of the proposed $G-\mu$ -S framework to the domain of Neurodevelopmental Disorders (NDDs). The aim is to offer a unifying theoretical perspective that conceptualizes NDDs as potential dysregulations of a self-regulatory dynamical system. By translating clinical phenomena into the formal language of bifurcations, attractors, and stability landscapes, the framework provides a generative foundation for hypothesis-driven research in computational psychiatry. It is important to clarify that this appendix does not aim to reduce NDDs deterministically; rather, it proposes a computational representation that can coexist with diverse neuropsychological models, assuming the heterogeneity of subtypes, developmental stages, and task dependencies. A summary of this interpretive direction is provided in Table 13.

Appendix C.2. A Dynamic Reinterpretation of NDDs

This section reinterprets characteristic features of major NDDs through the lens of Cognitive Phase Dynamics (CPD), moving beyond a purely parametric understanding of gain G and bias μ toward a structural account of internal dynamics. It should be emphasized that the following descriptions are heuristic in nature—intended to generate empirically testable hypotheses rather than to encompass the full clinical or etiological complexity of these conditions.

Appendix C.2.1. A State-Dominant Signature: Autism Spectrum Disorder (ASD)

One potential dynamic profile of Autism Spectrum Disorder (ASD) can be conceptualized as a tendency toward excessive state-dominance. This working hypothesis suggests that some features of ASD may correspond to a system with a chronically elevated CPD indicator ($D_{\text{CPD}} \gg 1$), reflecting disproportionately strong stabilizing forces in the symmetric component of the interaction matrix (\mathbf{W}_{Fe}). This could result in overly rigid attractor basins, providing a model for the cognitive and behavioral inflexibility that can typify ASD

Appendix C.2.2. A Process-Dominant Signature: Tic Disorders and Rumination

In contrast, some features of Tic Disorders can be approximated by a tendency toward excessive process-dominance. The involuntary, repetitive movements might be modeled as limit cycle-like dynamics emerging from a system with a low CPD indicator ($D_{\text{CPD}} \ll 1$). This view is consistent with dysregulations in cortico-basal ganglia-thalamo-cortical loops, where strong rotational forces could drive persistent looping activity. While this simple model does not capture the full phenomenology of premonitory urges and subsequent relief, it provides a potential dynamic substrate. The same mechanism may underlie cognitive phenomena such as rumination, which also reflect a failure to exit a recurrent process.

Appendix C.2.3. A Meta-Control Instability Signature: ADHD

Attention-Deficit/Hyperactivity Disorder (ADHD) can be interpreted as a case of instability in metacontrol. This hypothesis is complementary to other models of ADHD (e.g., executive function or delay aversion models). Within our framework, inattention could be conceptualized as a failure to sustain a state-dominant regime, while the phenomenon of hyperfocus, observed in some individuals, might correspond to a transient "lock-in" to an overly stable configuration. This perspective suggests a dysregulation within the self-system S, which is responsible for adaptively managing the balance between focused stability and flexible exploration.

Appendix C.3. Prospects for Hypothesis Testing and Intervention

This dynamic reinterpretation opens several promising directions for both theoretical and empirical investigation:

- Neural Correspondence: The search for neural correlates can be refined within this dynamical framework. For example, a high D_{CPD} in ASD may correspond to hyperconnectivity within specific cortical modules, whereas a low D_{CPD} in Tic Disorders may relate to dysregulated basal ganglia—thalamo—cortical loops.
- Model-Based Interventions: The effects of interventions could be retrospectively modeled and understood through this framework. For example, the clinical effects of pharmacological or psychotherapeutic treatments might be described as a shift in the estimated system parameters $(G, \sigma, \mathbf{W}_{Fe})$, allowing for a computational characterization of treatment response.
- Transdiagnostic Marker Candidates: The indicators D_{IDE} and D_{CPD} could serve as exploratory computational marker candidates. As such, they require rigorous psychometric validation (e.g., reliability and construct validity). A working hypothesis is that cognitive rigidity, a feature common to disorders like ASD and OCD, might correspond to an elevated D_{CPD} in specific cognitive subspaces.

Appendix C.4. Disclaimer

This appendix constitutes a theoretical exploration intended solely to illustrate the potential applications of the proposed framework. It does not constitute medical or psychological advice. The dynamical models of NDDs presented here are hypothetical and simplified representations; their clinical validity remains to be established through rigorous empirical investigation.